Synthesis and characterization of a bimetallic americium(III) pyrithionate coordination complex

Zachary K. Huffman,[a] Joseph M. Sperling,[a] Cory J. Windorff,[a,b] Brian N. Long,[a] Lucas Cordova,[a] Harry Ramanantoanina,[c] Cristian Celis-Barros,*[a] Thomas E. Albrecht-Schönzart*[a]

[a] Department of Chemistry and Biochemistry, Florida State University, 95 Chieftan Way, Tallahassee, Florida 32306, United States

[b] Department of Chemistry and Biochemistry, New Mexico State University, MSC 3C, PO Box 3001, Las Cruces, New Mexico 88003, United States

[c] Karlsruhe Institute of Technology, Institute for Nuclear Waste Disposal (INE), P.O. Box 3640, D-76021 Karlsruhe, Germany

Electronic Supplementary Information

Tables of Contents

Methods

Experimental

Considerations. CAUTION! ^{243}Am (t½ = 7370 years) is an α-particle emitting radioisotope that is hazardous to human health. Furthermore, the primary daughter isotope (^{239}Np) is a strong γ-ray emitter with high specific activity. All sample manipulations were conducted on an appropriately sized scale in a specially designated laboratory equipped with HEPA filtration.

Materials. All synthetic procedures were carried out in air with no attempt to exclude air or water in a well-ventilated fume hood in ambient conditions. The following solvents and chemicals were purchased reagent grade from commercial sources and used as received: HCl (concentrated, 37%, Sigma), HNO_3 (concentrated, ≥90%, Sigma), NH_3(aq) (concentrated, 28-30%, Sigma), Na(mpo) (Sigma-Aldrich, ≥96%). Deionized water was obtained from an in-house system. $LnCl_3$•$6H_2O$ and $Ln(NO_3)_3$•$6H_2O$ were prepared by dissolution of Ln_2O_3 (Sigma-Aldrich, Strem) in concentrated acid (Sigma-Aldrich), evaporation to dryness, washing with diethyl ether (≥99.0%, Sigma-Aldrich), and drying under house vacuum for 12 hours.

Instrumentation. Solid-state UV-vis-NIR spectra of single crystals were collected using a CRAIC Technologies UV-vis-NIR microspectrophotometer with a mercury light source. Single crystals were isolated on glass slides using Parabar 10312 immersion oil and data were collected from 350 to 1000 nm at room temperature.

Crystallographic diffraction data were collected by mounting single crystals on a MITOGEN MicroLoop LD and aligning with a digital camera on a Bruker D8 Quest X-ray diffractometer. Collections used Mo Kα X-rays (λ = 0.71073 Å) from an IμS X-ray source and collection strategies were calculated using the APEX III software.[1] Structures were solved using intrinsic phasing methods (SHELXT) and refined by least squares techniques (SHELXL) in the OLEX2 program.[2,3] Crystallographic data and parameters can be found below.

Synthesis.

General Synthesis of [Am(mpo)$_2$(μ-O-mpo)(H_2O)]$_2$•$3H_2O$, **1-Am**. An aliquot of ^{243}Am (5 mg of ^{243}Am content, 0.021 mmol) in 2 M HCl was reacted with excess $NH_{3(aq)}$ until a pale-yellow solid precipitated out of solution. Credulously identified as "$Am(OH)_3$," the precipitate was washed with DI water (2 × 3 mL) before being suspended in water (1 mL) and redissolved with concentrated HCl (1 mL). The resulting yellow solution was diluted to 5 mL with water and combined with Na(mpo) (10 mg, 0.067 mmol) dissolved in water (2.0 mL). Slow evaporation of the resulting solution over a period of 48 hours resulted in X-ray-quality crystals which were suitable for data collection. Due to radiological constraints, a final yield could not be determined.

General Synthesis of [Ln(mpo)$_2$(μ-O-mpo)(H_2O)]$_2$, **1-Ln** (Ln = La, Pr, Nd, Sm, Eu, Gd, Tb): $LnCl_3$•$6H_2O$ (0.055 mmol) or $Ln(NO_3)_3$•$5H_2O$ (0.055 mmol) in water (1.0 mL) was combined with Na(mpo) (25 mg, 0.17 mmol). Slow evaporation of the solution over a period of 24 hours

resulted in X-ray-quality crystals which were washed (2 × 3mL) with DI water followed by (2 × 3mL) diethyl ether prior to data collection.

1-[La(mpo)$_2$(μ-O-mpo)(H$_2$O)]$_2$

When $LaCl_3$•$6H_2O$ (18 mg) or $La(NO_3)_3$•$5(H_2O)$ (22 mg) was used, 1-**[La(mpo)$_2$(μ-O-mpo)(H$_2$O)]$_2$** was isolated as colorless crystals (yield 26 mg, 88%).

1-[Pr(mpo)$_2$(μ-O-mpo)(H$_2$O)]$_2$

When $PrCl_3$•$6H_2O$ (19 mg) or $Pr(NO_3)_3$•$5(H_2O)$ (23 mg) was used, 1-**[Pr(mpo)$_2$(μ-O-mpo)(H$_2$O)]$_2$** was isolated as green crystals (yield 25 mg, 87%). UV/vis/NIR [λ_{max}, nm, single crystal]: 452.9 $^3P_2$, 471.5 $^3P_1$, 489.4 $^3P_0$, 598.1 $^1D_2$.

1-[Nd(mpo)$_2$(μ-O-mpo)(H$_2$O)]$_2$

When $NdCl_3$•$6H_2O$ (19 mg) or $Nd(NO_3)_3$•$5(H_2O)$ (23 mg) was used, 1-**[Nd(mpo)$_2$(μ-O-mpo)(H$_2$O)]$_2$** was isolated as blue crystals (yield 26 mg, 88%). UV/vis/NIR [λ_{max}, nm, single crystal]: 431.0 $^2P_{1/2}$, 529.7 $^4G_{7/2}$, 589.7, 597.3 – both excitations are $^4G_{5/2}$ or $^4G_{7/2}$, 685.4 $^4F_{9/2}$, 738.4, 748.2, 758.7 – all excitations are $^4F_{7/2}$ or $^4S_{3/2}$, 802.8, 806.5 – both excitations are $^2H_{9/2}$ or $^4S_{3/2}$, 868.0 $^4F_{3/2}$.

1-[Sm(mpo)$_2$(μ-O-mpo)(H$_2$O)]$_2$

When $SmCl_3$•$6H_2O$ (20 mg) or $Sm(NO_3)_3$•$5(H_2O)$ (23 mg) was used, 1-**[Sm(mpo)$_2$(μ-O-mpo)(H$_2$O)]$_2$** was isolated as colorless crystals (yield 25 mg, 84%). UV/vis/NIR [λ_{max}, nm, single crystal]: 407.6 $^6P_{3/2}$, 423.2 – excitation is $^4F_{7/2}$ or $^4L_{13/2}$.

1-[Eu(mpo)$_2$(μ-O-mpo)(H$_2$O)]$_2$

When $EuCl_3$•$6H_2O$ (20 mg) or $Eu(NO_3)_3$•$5(H_2O)$ (24 mg) was used, 1-**[Eu(mpo)$_2$(μ-O-mpo)(H$_2$O)]$_2$** was isolated as orange crystals (yield 24 mg, 81%).

1-[Gd(mpo)$_2$(μ-O-mpo)(H$_2$O)]$_2$

When $GdCl_3$•$6H_2O$ (20 mg) or $Gd(NO_3)_3$•$5(H_2O)$ (24 mg) was used, 1-**[Gd(mpo)$_2$(μ-O-mpo)(H$_2$O)]$_2$** was isolated as colorless crystals (yield 25 mg, 83%).

1-[Tb(mpo)$_2$(μ-O-mpo)(H$_2$O)]$_2$

When $TbCl_3$•$6H_2O$ (21 mg) or $Tb(NO_3)_3$•$5(H_2O)$ (24 mg) was used, 1-**[Tb(mpo)$_2$(μ-O-mpo)(H$_2$O)]$_2$** was isolated as colorless crystals (yield 25 mg, 83%).

General Synthesis of Ln(mpo)$_3$(H$_2$O)$_2$•H$_2$O, **2-Ln** (Ln = Dy, Ho, Er, Tm, Yb, Lu): $LnCl_3$•$6H_2O$ (0.055 mmol) or $Ln(NO_3)_3$•$5H_2O$ (0.055 mmol) in water (1.0 mL) was combined with Na(mpo) (25 mg, 0.17 mmol). Slow evaporation of the solution over a period of 24 hours resulted in X-ray-quality crystals which were washed (2 × 3mL) with DI water followed by (2 × 3mL) diethyl ether prior to data collection.

2-Dy(mpo)$_3$(H$_2$O)$_2$•H$_2$O

When $DyCl_3$•$6H_2O$ (21 mg) or $Dy(NO_3)_3$•$5(H_2O)$ (24 mg) was used, 2-**Dy(mpo)$_3$(H$_2$O)$_2$•H$_2$O** was isolated as colorless crystals (yield 28 mg, 86%). UV/vis/NIR [λ_{max}, nm, single crystal]: 454 $^4I_{15/2}$, 760 $^6F_{3/2}$, 809 $^6F_{5/2}$, 916 $^6F_{7/2}$.

2-Ho(mpo)$_3$(H$_2$O)$_2$•H$_2$O

When $HoCl_3$•$6H_2O$ (21 mg) or $Ho(NO_3)_3$•$5(H_2O)$ (24 mg) was used, **2-Ho(mpo)$_3$(H$_2$O)$_2$•H$_2$O** was isolated as pink crystals (yield 27 mg, 82%). UV/vis/NIR [λ_{max}, nm, single crystal]: 415 $^5G_5$, 452, 456, 461 - all excitations are $^5F_1$ or $^5G_6$, 480 $^5F_3$, 538, 542 – both excitations are $^6F_{7/2}$ or $^5S_2$, 640 $^5F_5$.

2-Er(mpo)$_3$(H$_2$O)$_2$•H$_2$O

When $ErCl_3$•$6H_2O$ (21 mg) or $Er(NO_3)_3$•$5(H_2O)$ (24 mg) was used, **2-Er(mpo)$_3$(H$_2$O)$_2$•H$_2$O** was isolated as pink crystals (yield 29 mg, 88%). UV/vis/NIR [λ_{max}, nm, single crystal]: 489 $^5F_{7/2}$, 522 $^2H_{11/2}$, 543 $^4S_{3/2}$, 656 $^4F_{9/2}$.

2-Tm(mpo)$_3$(H$_2$O)$_2$•H$_2$O

When $TmCl_3$•$6H_2O$ (21 mg) or $Tm(NO_3)_3$•$5(H_2O)$ (25 mg) was used, **2-Tm(mpo)$_3$(H$_2$O)$_2$•H$_2$O** was isolated as colorless crystals (yield 27 mg, 82%). UV/vis/NIR [λ_{max}, nm, single crystal]: 473 $^1G_4$, 690 $^3F_3$, 795 $^3H_4$.

2-Yb(mpo)$_3$(H$_2$O)$_2$•H$_2$O

When $YbCl_3$•$6H_2O$ (21 mg) or $Yb(NO_3)_3$•$5(H_2O)$ (25 mg) was used, **2-Yb(mpo)$_3$(H$_2$O)$_2$•H$_2$O** was isolated as colorless crystals (yield 29 mg, 87%). UV/vis/NIR [λ_{max}, nm, single crystal]: 978 $^2F_{5/2}$.

2-Lu(mpo)$_3$(H$_2$O)$_2$•H$_2$O

When $LuCl_3$•$6H_2O$ (21 mg) or $Lu(NO_3)_3$•$5(H_2O)$ (25 mg) was used, **2-Lu(mpo)$_3$(H$_2$O)$_2$•H$_2$O** was isolated as colorless crystals (yield 28 mg, 84%).

Theory

Bonding. The electronic structure and bonding of **1-Nd** and **1-Am** were studied computationally based on the experimental crystal structures, where only hydrogen atoms were optimized to keep the constraints imposed by the crystal packing. A simple yet detailed analysis was performed to the full structures by localizing the molecular electron density from a density functional theory (DFT) calculation under the Natural Bond Orbital (NBO) formalism. All calculations were performed with the ADF engine in AMS 2021.106.[4] The hybrid generalized gradient approximation (GGA) functional PBE0 was used along with the Slater-type basis set of triple-ζ quality STO-TZP. Scalar-relativistic effects were included in the zeroth-order regular approximation (ZORA) to the Dirac equation.[5] For the free ligand geometry optimization, the GGA functional PBE was considered in conjunction with the STO-TZP basis set after which a single-point calculation was performed using the hybrid GGA PBE0 functional for comparable results. NBO calculations were performed with NBO 6,[6] which is coupled to ADF suite.

Ligand Field DFT. Given the Laporte forbidden nature of *f-f* transitions, reproducing and interpreting them in terms of wavefunction composition and transition intensities from first

principles present a challenge from a theoretical viewpoint. However, recent developments on ligand field density functional theory (LFDFT)[7] have allowed us to reproduce accurately the lower energy portion of **1-Am** (**Figure S22**). A modified version of the LFDFT in conjunction with the version implemented in ADF have been used to obtain the intensity of the *f-f* transitions. The ligand field parameters were obtained using the hybrid GGA functional PBE0 along with the STO-TZ2P for Am and TZP for the rest of the atoms. The HF exchange for these calculations was increased to 50% for a better prediction of the energy of the excited states.

The *f-f* transitions were calculated from first principles using the static approximation, i.e. no vibrational states were considered. The electric transition dipole moments were calculated in the dipole-length form according to $\mu = -r$, whereas the intensities associated with a particular electronic transition between states the initial state i and final state k were obtained from $f_{ik} = \frac{2}{3}\Delta E_{ik} < i|\mu|k >^2$.

Supplementary results and discussion

Spectroscopy. Solid-state spectra of **1-Ln** and **2-Ln** reveals a broad ligand-based transition that is generally centered about 360-390 nm and exhibit Laporte forbidden *f-f* transitions characteristic of the respective cation in an aqueous environment, see **Figures S1 – S9**. **1-Pr** shows hypersensitive transitions at 452.9 nm ($^3H_4 \rightarrow {}^3P_2$) and 598.1 nm ($^3H_4 \rightarrow {}^1D_2$), and **1-Nd** has hypersensitive transitions at 529.7 nm ($^4I_{9/2} \rightarrow {}^4G_{7/2}, {}^4K_{13/2}$) and 590.4 nm ($^4I_{9/2} \rightarrow {}^4G_{5/2}, {}^2G_{7/2}$), both a slight bathochromic shift compared to these transitions for the free ions.[8] **1-Sm** exhibits *f-f* transitions above the ligand-based transition centered about 380 nm where the most intense *f-f* transition at 407.6 nm ($^6H_{5/2} \rightarrow {}^6P_{7/2}, {}^4D_{1/2}, {}^4F_{9/2}$) is seen in the onset of the broad band. The *f-f* transitions for **1-Gd** are higher in energy than what is seen in the spectrum, and so only a broad band is observed. Monomeric pyrithionate compounds **2-Ln** similarly show typical *f-f* transitions above approximately 390 nm. Hypersensitive transitions are observed in **2-Ho** at 453.7 nm ($^5I_8 \rightarrow {}^5G_6$) as well as **2-Er** at 405 nm as a shoulder of the ligand-based transition onset and at 522.7 nm ($^4I_{15/2} \rightarrow {}^2H_{11/2}$). Likewise, **2-Tm** exhibits *f-f* transitions at 473.2 nm ($^3H_6 \rightarrow {}^1G_4$), 690.6 nm ($^3H_6 \rightarrow {}^3F_3$), and 795.5 nm ($^3H_6 \rightarrow {}^3H_4$).

While the colors of **1-Ln** and **2-Ln** are largely the same as those respective ions in aqueous solution, **1-Eu** and **2-Yb** appear orange and yellow in color, respectively. Solid-state absorption spectra of **1-Eu** (**Figure S4**) shows a charge transfer band centered about 424 nm and spectra of **2-Yb** (**Figure S9**)shows this charge transfer band centered at 401 nm, which are both marginally lower in energy than the LMCT band observed for isomorphous **1-Ln** and **2-Ln**. Spectra of **1-Eu** shows the absorption of more light in the region from 425-450 nm compared to **2-Yb**, resulting in the transmission of more orange light in **1-Eu** compared to **2-Yb**. While atypical for most Eu(III) and Yb(III) aqueous complexes this phenomenon has been reported elsewhere with ligands that feature soft donor atoms, namely dithiocarbamates.[9]

Only **1-Tb** exhibited phosphorescence of the lanthanide pyrithionate complexes, **Figure S10**, where excitation using 420 nm at 298 K showed transitions characteristic of Tb(III) at 490.2 nm ($^5D_4 \rightarrow {}^7F_6$), 544.3 nm ($^5D_4 \rightarrow {}^7F_5$), 586.6 nm ($^5D_4 \rightarrow {}^7F_4$), and 618.0 nm ($^5D_4 \rightarrow {}^7F_3$).

Bonding. Bond orders have been estimated with the Wiberg and NLMO approximations. The former is considered a standard approximation to estimate bond orders, whereas the latter distinguishes between bonding and antibonding interactions providing additional information of the bond. Furthermore, NLMO-based bond indices (NLMO-BI) can be decomposed in individual NLMO contributions that can be useful to identify the NLMOs that describe more appropriately the bond. **Table S30** summarizes the M–L (M = Nd, Eu, Am; L = S, O) bond orders predicted by both formalisms showing the expected trend, i.e. Am–L bonds are stronger than Ln–L bonds. Bridging O_{mpo} atoms show significantly weaker bonds (ΔWBI > 0.1) with respect to the other two non-bridging mpo ligands, which unexpectedly weakens the M–S coordination (ΔWBI > 0.1). This could relate to synergistic effects between the sulfur and oxygen atoms in mpo. This same trend is observed throughout the NLMO-BIs, though showing smaller values owing to the antibonding contributions to the bond order. Overall, the order of strength follows M–mpo3(6) > M–mpo2(5) > M–mpo1(4) (labels correspond to those of **Figure 3**).

Following the order of bond strength, M–O bonds also show differences among them, though mpo2 and mpo3 are not distinguishable as show for M–S bonds. Therefore, M–mpo2 and M–mpo3 bonds show similar bonding components including a σ– and a π–contribution with similar metal contributions (**Figure S19**). Interestingly, for the Am–O3 NLMOs, the 5*f* hybrid composition is significantly lower than even the Nd–O3 NLMOs, which is compensated by an increase of the 6*d* orbital contribution. Conversely, the double interaction of the bridging M–O bonds causes their NLMOs to differ from the other bonds, denoting the weaker interaction lacking of a significant π component. Similarly, the M–O_{water} bond compares to that of the bridges in terms of bond orders, which is also explained by the lack of a π–contribution that could reinforce the bond. Overall, the Eu – L bonds are slightly weaker than those of **1-Nd** with less involvement of the 4*f* shell. This might be attributed to the fact that the 4*f* shell is more shielded in Eu than Nd due to the progressive orbital contraction. Thus, comparing isovalent configurations such as Am and Eu highlights the difference in bonding in the same footing in terms of valence electrons.

Given the delocalized nature of the ligand (**Figure S19**), a final approach to study the metal–ligand interaction can be performed by scrutinizing the structural and electronic arrangements of the ligand upon complexation. The geometry of the mpo was optimized as a free ligand and compared to the average structures in the corresponding complexes. From the structural comparison, it is clear that the C–S and N–O distances elongate upon coordination, while the C–N bond contracts (**Table S31**). This suggests a weakening of the C–S and N–O because of the metal interaction that is compensated with a strengthening of the C–N bond, which is confirmed by calculated bond orders (**Table S32**). Our calculated values suggest an increase in the C–N WBIs by > 0.1 and a decreased in the C–S and N–O WBIs by ~ 0.1 and ~ 0.2, respectively. Furthermore, the stabilization coming from the delocalization of on sulfur lone pair (LP) to an antibonding N–O NBO in the form of a hyperbond (3-center 4-electron interaction) observed in the free ligand is completely altered upon coordination where a different sulfur LP is significantly delocalized toward the C–N bond. This supports and provides an explanation to the observed structural and electronic changes in the ligand because of the metal ligation.

While the hydroxamic acid motif has been heavily studied for decades across the *f*-block, this body of work aims to show the potential behind the five-membered ring encountered in hydroxamate coordination complexes and that it can be tuned using differing donor atoms to selectively bind a variety of metal ions. Thioamides specifically have been largely neglected in the chelation of *f*-elements and herein we show that pyrithione displays considerable electronic variation upon coordination with respect to specific cations in the *f*-block.

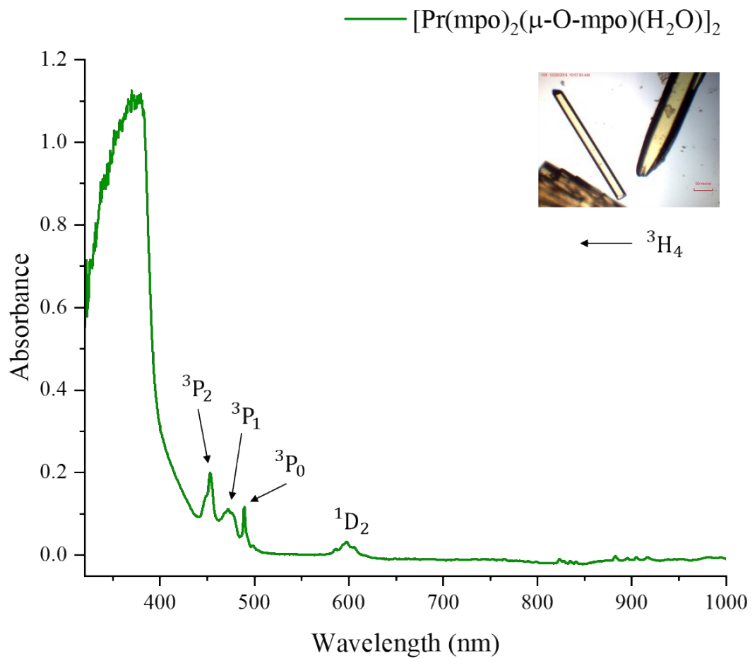

Figure S1, <u>1-Pr</u>: Solid state UV-vis/NIR absorption spectra of $[Pr(mpo)_2(\mu\text{-O-mpo})(H_2O)]_2$.

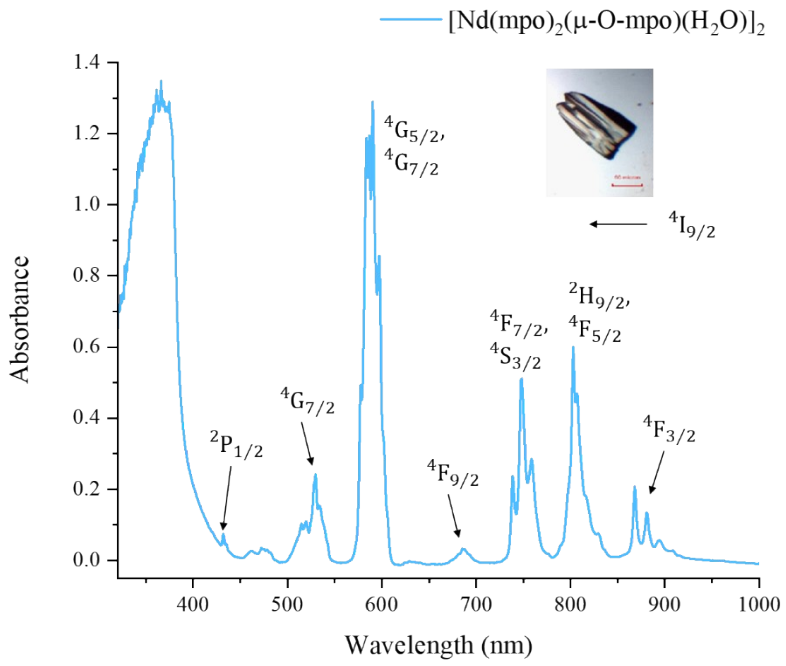

Figure S2, <u>1-Nd</u>: Solid state UV-vis/NIR absorption spectrum of $[Nd(mpo)_2(\mu\text{-O-mpo})(H_2O)]_2$.

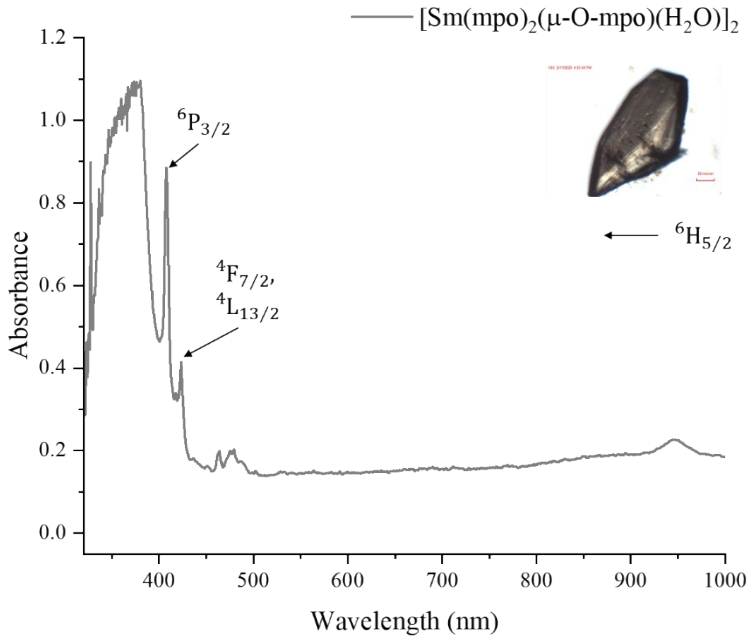

Figure S3, <u>1-Sm</u>: Solid state UV-vis/NIR absorption spectrum of $[Sm(mpo)_2(\mu\text{-O-mpo})(H_2O)]_2$.

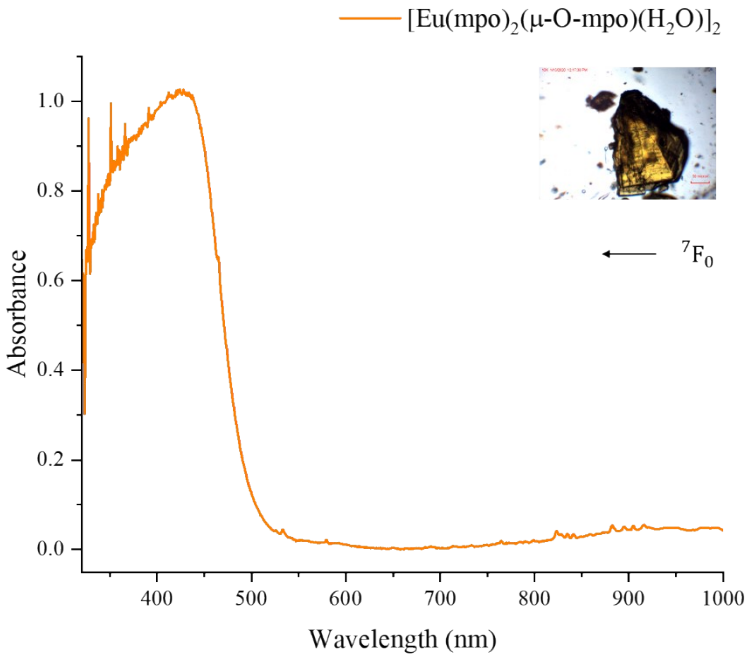

Figure S4, <u>1-Eu</u>: Uv-vis/NIR absorption spectrum of $[Eu(mpo)_2(\mu\text{-O-mpo})(H_2O)]_2$.

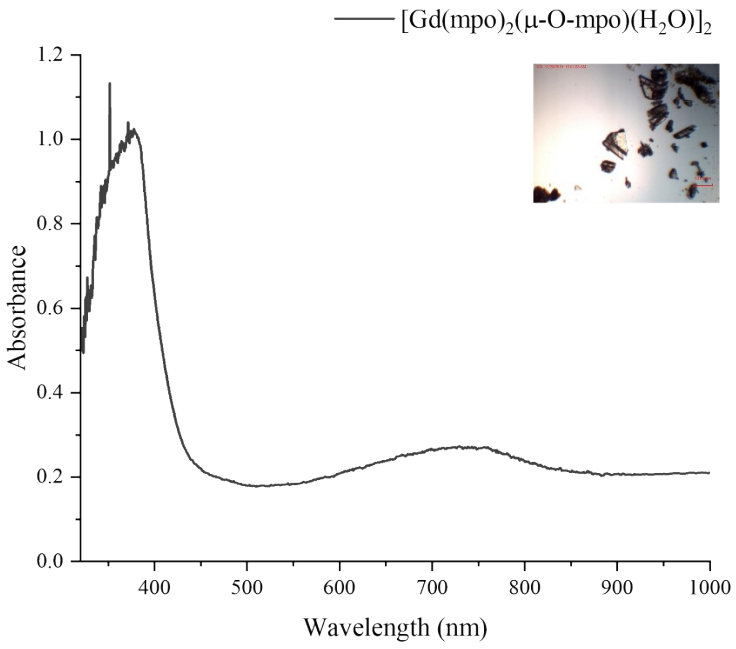

Figure S5, <u>1-Gd</u>: Uv-vis/NIR absorption spectrum of $[Gd(mpo)_2(\mu\text{-O-mpo})(H_2O)]_2$.

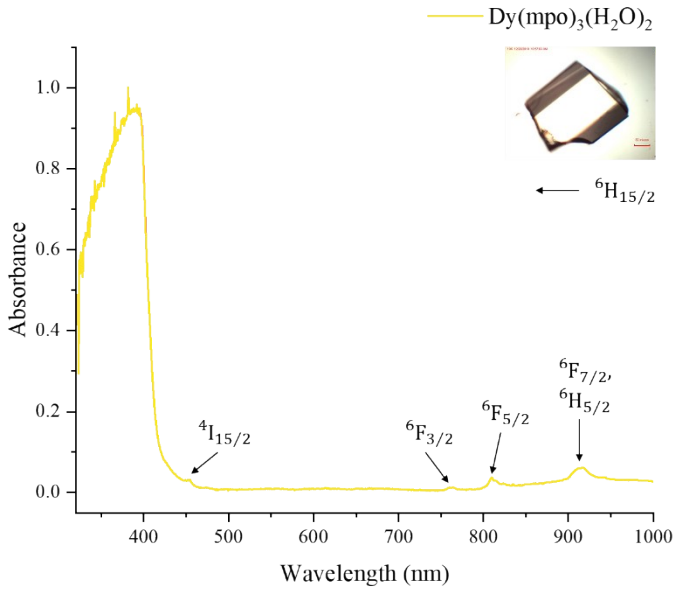

Figure S6, <u>2-Dy</u>: UV-vis/NIR absorption spectrum of $Dy(mpo)_3(H_2O)_2 \bullet H_2O$.

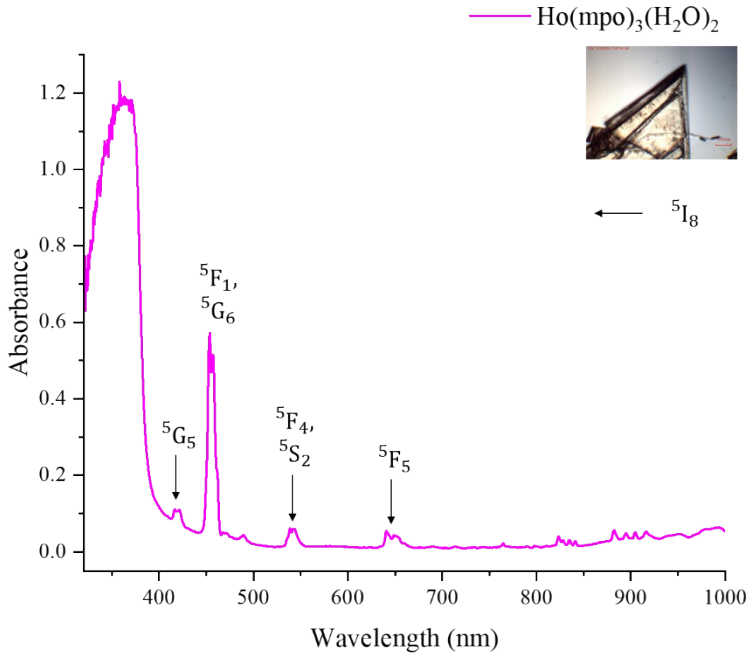

Figure S7, <u>2-Ho</u>: UV-vis/NIR absorption spectra of $Ho(mpo)_3(H_2O)_2 \bullet H_2O$.

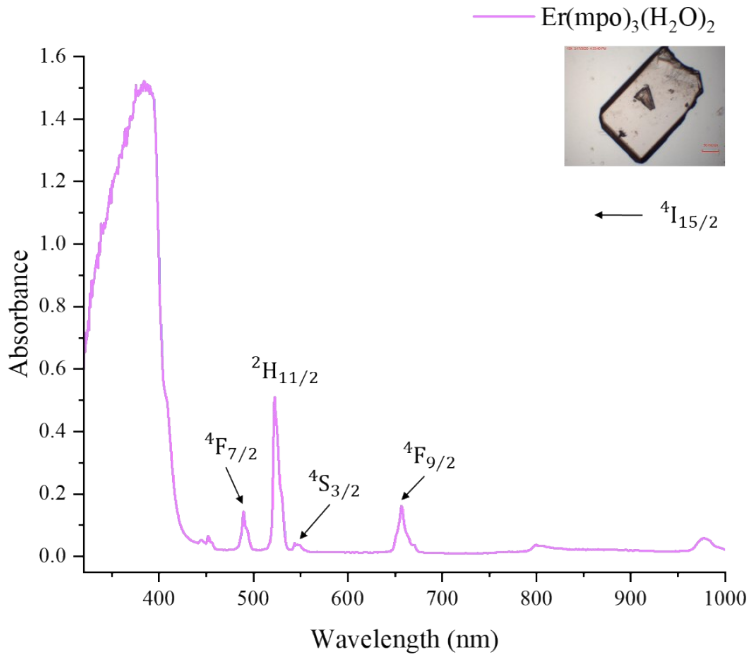

Figure S8, <u>2-Er</u>: UV-vis/NIR absorption spectra of $Er(mpo)_3(H_2O)_2 \bullet H_2O$.

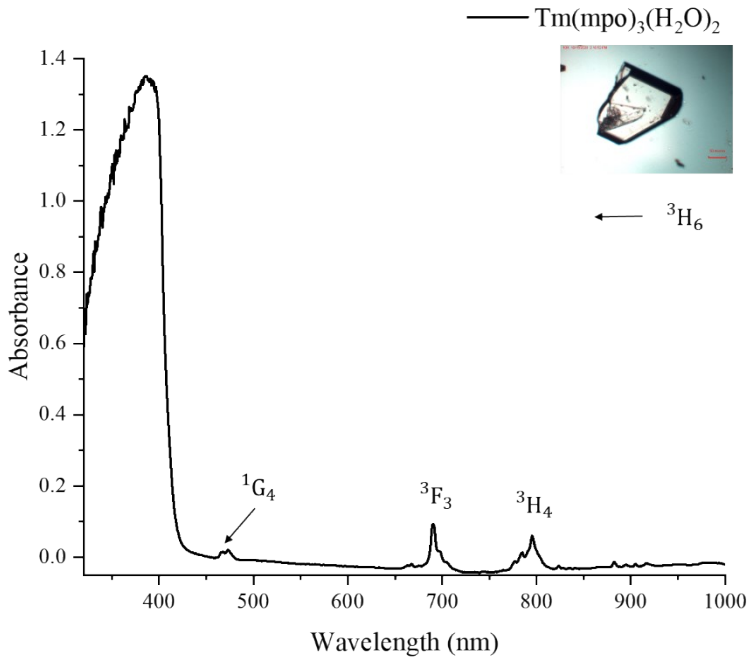

Figure S9, <u>2-Tm</u>: UV-vis/NIR absorption spectra of $Tm(mpo)_3(H_2O)_2 \bullet H_2O$.

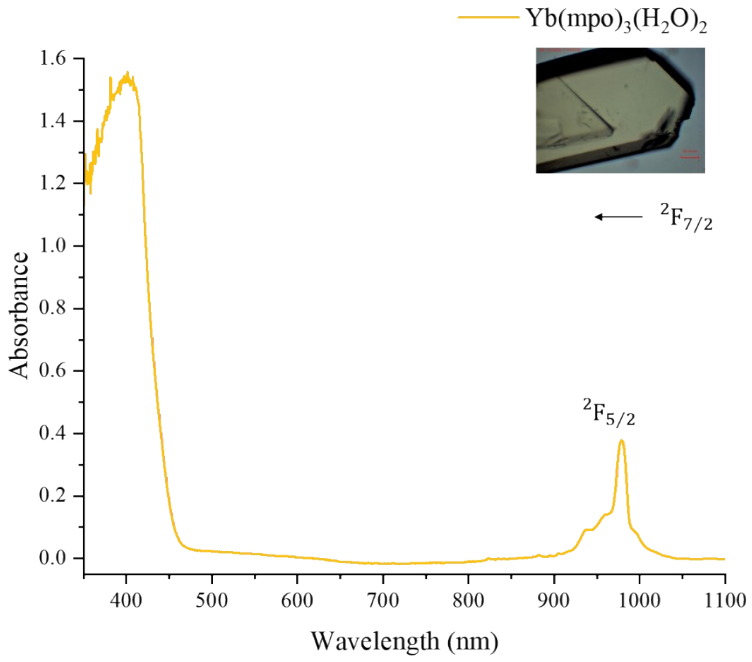

Figure S10, <u>2-Yb</u>: UV-vis/NIR absorption spectra of $Yb(mpo)_3(H_2O)_2 \bullet H_2O$.

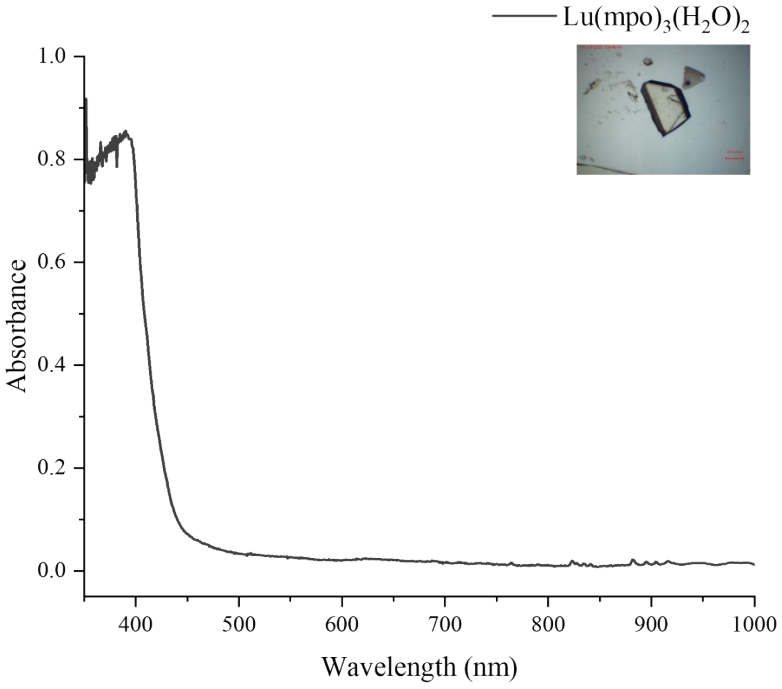

Figure S11, <u>2-Lu</u>: UV-vis/NIR absorption spectra of $Lu(mpo)_3(H_2O)_2 \bullet H_2O$.

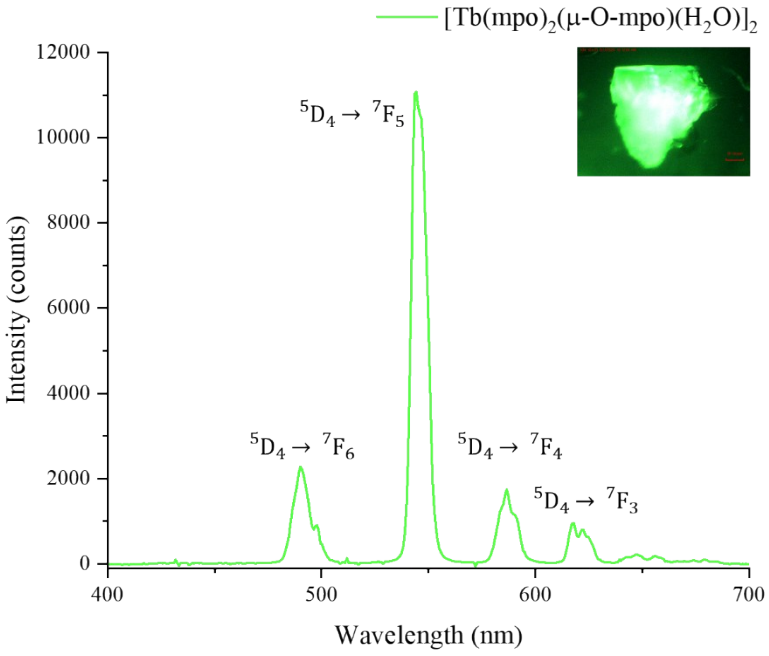

Figure S12, <u>1-Tb</u>: Phosphorescence of $[Tb(mpo)_2(\mu\text{-O-mpo})(H_2O)]_2$ at 298 K with 420 nm excitation.

Table S1. Selected bond lengths for the **1-Am** complex. Labels correspond to those shown in **Figure 3**.

	S1	S2	S3	O1	O2	O3
Am	2.946(2)	2.889(2)	2.873(2)	2.470(4)	2.368(4)	2.357(4)

Table S2. Selected averaged bond distances for $[M(mpo)_2(\mu\text{-O-mpo})(H_2O)]_2$.

1-M	**Pr**	**Nd**	**Sm**	**Eu**	**Gd**	**Tb**	**Am**
6-coordinate ionic radii	0.99	0.983	0.958	0.947	0.938	0.923	0.975
Ln-O_{mpo} (Å)	2.403(2)	2.393 (2)	2.363(2)	2.354 (2)	2.348 (1)	2.338 (1)	2.398 (2)
Ln-S (Å)	2.952(1)	2.934 (1)	2.908(1)	2.899 (1)	2.886 (2)	2.886 (2)	2.903 (1)
$M-M\ dist$	4.293 (3)	4.272 (2)	4.222 (5)	4.207 (5)	4.187 (3)	4.179 (8)	4.255 (4)

Table S3: Selected averaged bond distances for **2-Ln**.

1-Ln	**Dy**	**Ho**	**Er**	**Tm**	**Yb**	**Lu**
6-coordinate ionic radii	0.912	0.901	0.890	0.880	0.868	0.861
Ln-S (Å)	2.829(1)	2.818(1)	2.801(1)	2.796(1)	2.784(1)	2.775(1)
Ln-O_{mpo} (Å)	2.343(2)	2.333(2)	2.322(2)	2.314(2)	2.301(2)	2.295(2)

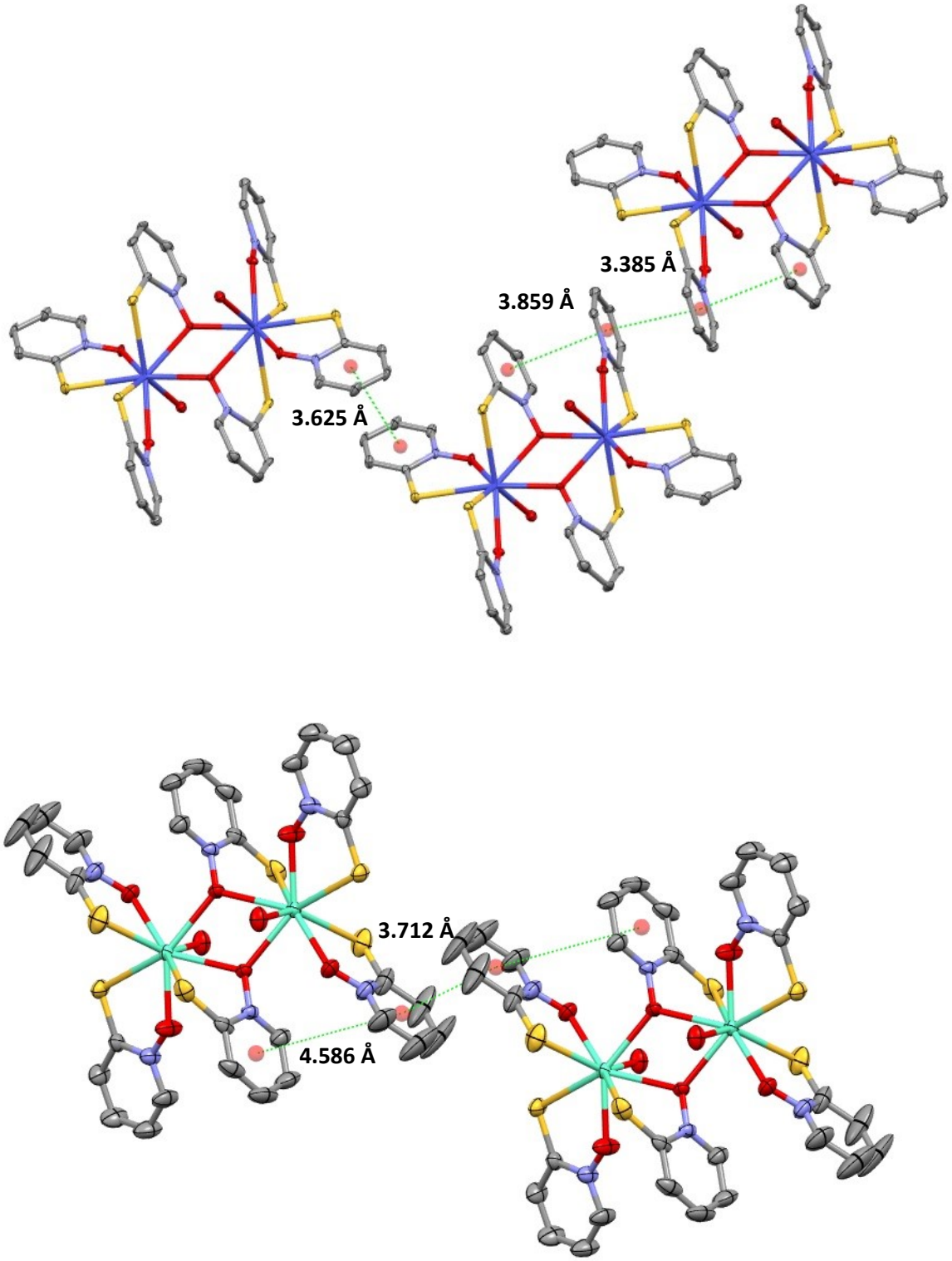

Figure S13: Crystal packing of **1-Am** (top) and **1-Nd** (bottom) where solvent molecules and hydrogens are omitted for clarity.

Crystallographic Data

Table S4 Crystal data and structure refinement for $[Pr(mpo)_2(\mu\text{-O-mpo})(H_2O)]_2$	
Empirical formula	$C_{15}H_{14}N_3O_4PrS_3$
Formula weight	537.38
Temperature/K	296.15
Crystal system	monoclinic
Space group	$P2_1/c$
a/Å	10.1531(2)
b/Å	10.0034(2)
c/Å	19.5478(5)
α/°	90
β/°	95.0440(10)
γ/°	90
Volume/Å^3	1977.69(8)
Z	4
ρcalcg/cm^3	1.805
μ/mm^{-1}	2.804
F(000)	1056.0
Crystal size/mm^3	0.419 × 0.22 × 0.193
Radiation	MoK_α (λ = 0.71073)
2Θ range for data collection/°	4.028 to 74.48
Index ranges	$-17 \leq h \leq 17$, $-17 \leq k \leq 17$, $-33 \leq l \leq 33$
Reflections collected	107132
Independent reflections	10213 [Rint = 0.0640, Rsigma = 0.0349]
Data/restraints/parameters	10213/0/236
Goodness-of-fit on F^2	1.029
Final R indexes [I≥2σ (I)]	R1 = 0.0351, wR2 =0.0654
Final R indexes [all data]	R1 = 0.0573, wR2 = 0.0728
Largest diff. peak/hole / e Å^{-3}	0.81/-1.24

Table S5 Bond Lengths for $[Pr(mpo)_2(\mu\text{-O-mpo})(H_2O)]_2$

Atom	Atom	Length/Å	Atom	Atom	Length/Å
Pr1	S1	2.9604(6)	N1	C1	1.357(3)
Pr1	S3	2.9979(6)	N1	C5	1.351(3)
Pr1	S2	2.8993(8)	N2	C6	1.355(5)
Pr1	O31	2.5143(15)	N2	C10	1.360(5)
Pr1	O3	2.5183(14)	C15	C14	1.372(4)
Pr1	O4	2.4669(18)	C1	C2	1.393(3)
Pr1	O2	2.3407(16)	C11	C12	1.409(3)
Pr1	O1	2.3538(18)	C5	C4	1.352(4)
S1	C1	1.708(2)	C14	C13	1.378(6)
S3	C11	1.719(3)	C2	C3	1.368(4)
S2	C6	1.710(4)	C12	C13	1.365(5)
O3	N3	1.358(2)	C4	C3	1.381(4)
O2	N2	1.324(3)	C6	C7	1.407(5)
N3	C15	1.346(3)	C10	C9	1.367(7)
N3	C11	1.360(3)	C7	C8	1.354(9)
O1	N1	1.329(3)	C9	C8	1.347(11)

[1]1-X,1-Y,1-Z

Table S6 Crystal data and structure refinement for $[Nd(mpo)_2(\mu\text{-O-mpo})(H_2O)]_2$	
Empirical formula	$C_{15}H_{14}N_3NdO_4S_3$
Formula weight	540.71
Temperature/K	296.15
Crystal system	monoclinic
Space group	$P2_1/c$
a/Å	10.1252(2)
b/Å	9.9839(2)
c/Å	19.5248(5)
α/°	90
β/°	95.0050(10)
γ/°	90
Volume/Å^3	1966.22(7)
Z	4
ρcalcg/cm^3	1.827
μ/mm^{-1}	2.984
F(000)	1060.0
Crystal size/mm^3	0.277 × 0.243 × 0.158
Radiation	MoK$_\alpha$ (λ = 0.71073)
2Θ range for data collection/°	4.038 to 82.254
Index ranges	-18 ≤ h ≤ 18, -18 ≤ k ≤ 18, -36 ≤ l ≤ 36
Reflections collected	112293
Independent reflections	13041 [Rint = 0.0411, Rsigma = 0.0233]
Data/restraints/parameters	13041/0/236
Goodness-of-fit on F^2	1.176
Final R indexes [I>=2σ (I)]	R1 = 0.0383, wR2 =0.0805
Final R indexes [all data]	R1 = 0.0467, wR2 = 0.0847
Largest diff. peak/hole / e Å^{-3}	1.45/-2.04

Table S7 Bond Lengths for $[Nd(mpo)_2(\mu\text{-O-mpo})(H_2O)]_2$

Atom	Atom	Length/Å	Atom	Atom	Length/Å
Nd1	S1	2.9450(5)	N1	C1	1.358(3)
Nd1	S3	2.9800(6)	N1	C5	1.353(3)
Nd1	S2	2.8790(8)	N2	C6	1.359(5)
Nd1	O31	2.5013(13)	N2	C10	1.358(5)
Nd1	O3	2.5026(13)	C15	C14	1.380(4)
Nd1	O4	2.4472(18)	C1	C2	1.400(3)
Nd1	O2	2.3335(16)	C11	C12	1.409(3)
Nd1	O1	2.3441(18)	C14	C13	1.372(6)
S1	C1	1.708(2)	C12	C13	1.364(5)
S3	C11	1.718(3)	C2	C3	1.370(4)
S2	C6	1.707(4)	C5	C4	1.355(4)
O3	N3	1.3540(19)	C3	C4	1.379(4)
O2	N2	1.323(3)	C6	C7	1.405(4)
N3	C15	1.350(3)	C10	C9	1.365(7)
N3	C11	1.365(3)	C9	C8	1.336(12)
O1	N1	1.322(2)	C7	C8	1.365(10)

[1]1-X,1-Y,1-Z

Table S8 Crystal data and structure refinement for $[Sm(mpo)_2(\mu\text{-O-mpo})(H_2O)]_2$	
Empirical formula	$C_{15}H_{14}N_3O_4S_3Sm$
Formula weight	546.82
Temperature/K	273.15
Crystal system	monoclinic
Space group	$P2_1/c$
a/Å	10.0701(15)
b/Å	9.9650(14)
c/Å	19.421(3)
α/°	90
β/°	94.919(4)
γ/°	90
Volume/Å^3	1941.7(5)
Z	4
ρcalcg/cm^3	1.871
μ/mm^{-1}	3.372
F(000)	1068.0
Crystal size/mm^3	0.487 × 0.163 × 0.148
Radiation	MoK_α (λ = 0.71073)
2Θ range for data collection/°	4.598 to 58.008
Index ranges	$-13 \le h \le 13$, $-13 \le k \le 13$, $-26 \le l \le 26$
Reflections collected	88915
Independent reflections	5167 [Rint = 0.0582, Rsigma = 0.0216]
Data/restraints/parameters	5167/0/236
Goodness-of-fit on F^2	1.106
Final R indexes [I>=2σ (I)]	R1 = 0.0296, wR2 =0.0666
Final R indexes [all data]	R1 = 0.0389, wR2 = 0.0719
Largest diff. peak/hole / e Å^{-3}	0.96/-0.52

Table S9 Bond Lengths for $[Sm(mpo)_2(\mu\text{-O-mpo})(H_2O)]_2$

Atom	Atom	Length/Å	Atom	Atom	Length/Å
Sm1	S1	2.9209(9)	N1	C1	1.355(4)
Sm1	S3	2.9527(10)	N1	C5	1.355(5)
Sm1	S2	2.8502(12)	N2	C6	1.353(7)
Sm1	O31	2.470(2)	N2	C10	1.351(6)
Sm1	O3	2.472(2)	C15	C14	1.371(6)
Sm1	O4	2.415(2)	C14	C13	1.369(8)
Sm1	O2	2.306(2)	C11	C12	1.410(5)
Sm1	O1	2.313(3)	C1	C2	1.409(5)
S1	C1	1.705(4)	C12	C13	1.368(7)
S3	C11	1.717(4)	C6	C7	1.407(6)
S2	C6	1.706(6)	C2	C3	1.361(6)
O3	N3	1.359(3)	C5	C4	1.352(6)
O2	N2	1.324(4)	C10	C9	1.347(8)
N3	C15	1.346(5)	C3	C4	1.377(6)
N3	C11	1.355(5)	C7	C8	1.373(11)
N1	O1	1.322(4)	C9	C8	1.338(13)

[1]1-X,1-Y,1-Z

Table S10 Crystal data and structure refinement for $[Eu(mpo)_2(\mu\text{-O-mpo})(H_2O)]_2$	
Empirical formula	$C_{15}H_{14}EuN_3O_4S_3$
Formula weight	548.43
Temperature/K	273.15
Crystal system	monoclinic
Space group	$P2_1/c$
a/Å	10.0543(13)
b/Å	9.9635(13)
c/Å	19.422(3)
α/°	90
β/°	94.902(4)
γ/°	90
Volume/Å^3	1938.5(4)
Z	4
ρcalcg/cm^3	1.879
μ/mm^{-1}	3.583
F(000)	1072.0
Crystal size/mm^3	0.359 × 0.158 × 0.148
Radiation	MoK_α (λ = 0.71073)
2Θ range for data collection/°	4.598 to 56.664
Index ranges	$-13 \le h \le 13$, $-13 \le k \le 13$, $-25 \le l \le 25$
Reflections collected	83814
Independent reflections	4822 [Rint = 0.0500, Rsigma = 0.0185]
Data/restraints/parameters	4822/0/236
Goodness-of-fit on F^2	1.127
Final R indexes [I>=2σ (I)]	R1 = 0.0253, wR2 =0.0477
Final R indexes [all data]	R1 = 0.0335, wR2 = 0.0511
Largest diff. peak/hole / e Å^{-3}	0.82/-0.62

Table S11 Bond Lengths for $[Eu(mpo)_2(\mu\text{-O-mpo})(H_2O)]_2$

Atom	Atom	Length/Å	Atom	Atom	Length/Å
Eu01	Eu011	4.2072(5)	N1	C1	1.356(4)
Eu01	S1	2.9118(8)	N1	C5	1.354(4)
Eu01	S3	2.9438(9)	N2	C6	1.357(5)
Eu01	S2	2.8407(11)	N2	C10	1.355(5)
Eu01	O31	2.4631(19)	C15	C14	1.374(5)
Eu01	O3	2.4623(19)	C14	C13	1.373(7)
Eu01	O2	2.296(2)	C1	C2	1.405(4)
Eu01	O4	2.405(2)	C5	C4	1.351(5)
Eu01	O1	2.306(2)	C11	C12	1.405(4)
S1	C1	1.704(3)	C12	C13	1.368(6)
S3	C11	1.722(4)	C2	C3	1.370(5)
S2	C6	1.714(5)	C6	C7	1.399(6)
O3	N3	1.359(3)	C10	C9	1.355(7)
O2	N2	1.328(4)	C4	C3	1.382(5)
N3	C15	1.344(4)	C9	C8	1.354(10)
N3	C11	1.361(4)	C7	C8	1.366(9)
O1	N1	1.322(3)			

[1]1-X,1-Y,1-Z

Table S12 Crystal data and structure refinement for $[Gd(mpo)_2(\mu\text{-O-mpo})(H_2O)]_2$	
Empirical formula	$C_{15}H_{14}GdN_3O_4S_3$
Formula weight	553.72
Temperature/K	273.15
Crystal system	monoclinic
Space group	$P2_1/c$
a/Å	10.0345(7)
b/Å	9.9366(7)
c/Å	19.3797(13)
α/°	90
β/°	94.848(2)
γ/°	90
Volume/Å^3	1925.4(2)
Z	4
ρcalcg/cm^3	1.910
μ/mm^{-1}	3.795
F(000)	1076.0
Crystal size/mm^3	0.915 × 0.371 × 0.218
Radiation	MoK$_\alpha$ (λ = 0.71073)
2Θ range for data collection/°	5.612 to 65.52
Index ranges	$-15 \le h \le 15$, $-15 \le k \le 15$, $-29 \le l \le 29$
Reflections collected	96150
Independent reflections	6892 [Rint = 0.0512, Rsigma = 0.0279]
Data/restraints/parameters	6892/54/236
Goodness-of-fit on F^2	1.091
Final R indexes [I>=2σ (I)]	R1 = 0.0336, wR2 =0.0569
Final R indexes [all data]	R1 = 0.0532, wR2 = 0.0628
Largest diff. peak/hole / e Å^{-3}	1.22/-0.66

Table S13 Bond Lengths for $[Gd(mpo)_2(\mu\text{-O-mpo})(H_2O)]_2$

Atom	Atom	Length/Å	Atom	Atom	Length/Å
Gd1	S1	2.9034(8)	N2	C10	1.352(5)
Gd1	S3	2.9316(8)	N2	C6	1.355(6)
Gd1	S2	2.8241(10)	N1	C1	1.355(4)
Gd1	O31	2.4484(18)	N1	C5	1.353(4)
Gd1	O3	2.4511(18)	C15	C14	1.364(5)
Gd1	O2	2.293(2)	C14	C13	1.372(7)
Gd1	O4	2.386(2)	C12	C11	1.407(4)
Gd1	O1	2.296(2)	C12	C13	1.364(6)
S1	C1	1.708(3)	C1	C2	1.397(4)
S3	C11	1.720(4)	C5	C4	1.354(5)
S2	C6	1.711(5)	C10	C9	1.350(7)
O3	N3	1.360(3)	C6	C7	1.403(6)
O2	N2	1.327(4)	C2	C3	1.364(5)
N3	C15	1.347(4)	C4	C3	1.378(5)
N3	C11	1.358(4)	C9	C8	1.352(10)
O1	N1	1.321(3)	C7	C8	1.357(9)

[1]1-X,1-Y,1-Z

Table S14 Crystal data and structure refinement for $[Tb(mpo)_2(\mu\text{-O-mpo})(H_2O)]_2$	
Empirical formula	$C_{15}H_{14}N_3O_4S_3Tb$
Formula weight	555.39
Temperature/K	273.15
Crystal system	monoclinic
Space group	$P2_1/c$
a/Å	10.061(3)
b/Å	9.949(3)
c/Å	19.421(5)
α/°	90
β/°	94.797(7)
γ/°	90
Volume/Å^3	1937.2(9)
Z	4
ρcalcg/cm^3	1.904
μ/mm^{-1}	3.999
F(000)	1080.0
Crystal size/mm^3	0.422 × 0.246 × 0.203
Radiation	MoK_α (λ = 0.71073)
2Θ range for data collection/°	5.602 to 55.174
Index ranges	$-13 \le h \le 13$, $-12 \le k \le 12$, $-25 \le l \le 25$
Reflections collected	101200
Independent reflections	4455 [Rint = 0.0331, Rsigma = 0.0097]
Data/restraints/parameters	4455/0/240
Goodness-of-fit on F^2	1.149
Final R indexes [I>=2σ (I)]	R1 = 0.0183, wR2 =0.0442
Final R indexes [all data]	R1 = 0.0194, wR2 = 0.0452
Largest diff. peak/hole / e Å^{-3}	0.49/-0.83

Table S15 Bond Lengths for $[Tb(mpo)_2(\mu\text{-O-mpo})(H_2O)]_2$

Atom	Atom	Length/Å	Atom	Atom	Length/Å
Tb1	S1	2.9083(9)	N1	C1	1.359(3)
Tb1	S3	2.9334(9)	N1	C5	1.357(3)
Tb1	S2	2.8169(10)	N2	C6	1.359(4)
Tb1	O3	2.4457(16)	N2	C10	1.357(4)
Tb1	O31	2.4473(16)	C15	C14	1.381(4)
Tb1	O4	2.3799(18)	C1	C2	1.417(3)
Tb1	O2	2.2836(17)	C2	C3	1.370(4)
Tb1	O1	2.285(2)	C11	C12	1.409(4)
S1	C1	1.706(2)	C12	C13	1.369(5)
S3	C11	1.725(3)	C14	C13	1.381(6)
S2	C6	1.719(4)	C3	C4	1.384(4)
O3	N3	1.361(2)	C5	C4	1.358(4)
O2	N2	1.332(3)	C6	C7	1.405(4)
N3	C15	1.348(3)	C10	C9	1.366(6)
N3	C11	1.366(3)	C7	C8	1.367(7)
O1	N1	1.330(3)	C9	C8	1.348(9)

[1]1-X,1-Y,1-Z

Table S16 Crystal data and structure refinement for $Dy(mpo)_3(H_2O)_2 \cdot H_2O$

Empirical formula	$C_{15}H_{18}DyN_3O_6S_3$
Formula weight	595.00
Temperature/K	296.15
Crystal system	triclinic
Space group	$P\bar{1}$
a/Å	7.4805(9)
b/Å	11.1541(15)
c/Å	13.1843(17)
α/°	111.472(3)
β/°	93.931(3)
γ/°	91.055(3)
Volume/Å^3	1020.2(2)
Z	2
ρcalcg/cm^3	1.937
μ/mm^{-1}	4.006
F(000)	582.0
Crystal size/mm^3	0.668 × 0.334 × 0.182
Radiation	MoK_α (λ = 0.71073)
2Θ range for data collection/°	5.464 to 67.152
Index ranges	-11 ≤ h ≤ 11, -17 ≤ k ≤ 17, -20 ≤ l ≤ 20
Reflections collected	58168
Independent reflections	7556 [Rint = 0.0650, Rsigma = 0.0331]
Data/restraints/parameters	7556/1/260
Goodness-of-fit on F^2	1.121
Final R indexes [I>=2σ (I)]	R1 = 0.0312, wR2 =0.0722
Final R indexes [all data]	R1 = 0.0385, wR2 = 0.0771
Largest diff. peak/hole / e Å^{-3}	1.58/-1.94

Table S17 Bond Lengths for $Dy(mpo)_3(H_2O)_2 \cdot H_2O$

Atom	Atom	Length/Å	Atom	Atom	Length/Å
Dy01	S2	2.7998(9)	N1	C1	1.372(4)
Dy01	S3	2.8642(9)	N1	C5	1.363(4)
Dy01	S1	2.8246(9)	N2	C6	1.379(4)
Dy01	O1	2.343(2)	N2	C10	1.357(4)
Dy01	O2	2.360(2)	C1	C2	1.411(4)
Dy01	O5	2.392(2)	C11	C12	1.418(5)
Dy01	O4	2.389(2)	C15	C14	1.370(6)
Dy01	O3	2.335(2)	C6	C7	1.401(5)
S2	C6	1.712(4)	C5	C4	1.367(5)
S3	C11	1.705(4)	C2	C3	1.373(6)
S1	C1	1.714(3)	C14	C13	1.384(8)
O1	N1	1.349(3)	C12	C13	1.370(7)
O2	N2	1.347(3)	C4	C3	1.389(6)
O3	N3	1.348(3)	C10	C9	1.370(5)
N3	C11	1.370(4)	C7	C8	1.367(7)
N3	C15	1.359(4)	C8	C9	1.386(7)

Table S18 Crystal data and structure refinement for $Ho(mpo)_3(H_2O)_2 \cdot H_2O$

Empirical formula	$C_{15}H_{18}HoN_3O_6S_3$
Formula weight	597.43
Temperature/K	296.15
Crystal system	triclinic
Space group	$P\bar{1}$
a/Å	7.4507(8)
b/Å	11.1249(13)
c/Å	13.1555(16)
α/°	111.452(3)
β/°	93.982(3)
γ/°	91.030(3)
Volume/Å^3	1011.3(2)
Z	2
ρcalcg/cm^3	1.962
μ/mm^{-1}	4.258
F(000)	584.0
Crystal size/mm^3	0.425 × 0.237 × 0.115
Radiation	MoK_α (λ = 0.71073)
2Θ range for data collection/°	5.486 to 56.464
Index ranges	$-8 \le h \le 9$, $-14 \le k \le 14$, $-16 \le l \le 17$
Reflections collected	32658
Independent reflections	4439 [Rint = 0.0586, Rsigma = 0.0416]
Data/restraints/parameters	4439/1/260
Goodness-of-fit on F^2	1.131
Final R indexes [I>=2σ (I)]	R1 = 0.0269, wR2 =0.0457
Final R indexes [all data]	R1 = 0.0402, wR2 = 0.0486
Largest diff. peak/hole / e Å^{-3}	0.84/-0.92

Table S19 Bond Lengths for $Ho(mpo)_3(H_2O)_2 \cdot H_2O$

Atom	Atom	Length/Å	Atom	Atom	Length/Å
Ho01	S3	2.8522(9)	N2	C6	1.371(4)
Ho01	S1	2.7847(9)	N2	C10	1.353(4)
Ho01	S2	2.8108(9)	N1	C1	1.367(4)
Ho01	O1	2.344(2)	N1	C5	1.354(4)
Ho01	O2	2.330(2)	C11	C12	1.401(5)
Ho01	O4	2.366(2)	C6	C7	1.406(5)
Ho01	O5	2.370(2)	C10	C9	1.358(5)
Ho01	O3	2.321(2)	C15	C14	1.362(5)
S3	C11	1.707(4)	C1	C2	1.405(5)
S1	C1	1.709(4)	C5	C4	1.361(5)
S2	C6	1.708(4)	C14	C13	1.379(6)
O1	N1	1.349(3)	C12	C13	1.357(6)
O2	N2	1.349(3)	C7	C8	1.360(5)
O3	N3	1.344(3)	C9	C8	1.385(5)
N3	C11	1.370(4)	C2	C3	1.360(6)
N3	C15	1.351(4)	C4	C3	1.374(6)

Table S20 Crystal data and structure refinement for $Er(mpo)_3(H_2O)_2 \cdot H_2O$

Empirical formula	$C_{30}H_{36}Er_2N_6O_{12}S_6$
Formula weight	1199.53
Temperature/K	296.15
Crystal system	triclinic
Space group	$P\bar{1}$
a/Å	7.44370(10)
b/Å	11.0980(2)
c/Å	13.1205(2)
α/°	111.4100(10)
β/°	94.0230(10)
γ/°	91.0700(10)
Volume/Å^3	1005.46(3)
Z	1
ρcalcg/cm^3	1.981
μ/mm^{-1}	4.522
F(000)	586.0
Crystal size/mm^3	0.563 × 0.34 × 0.258
Radiation	MoK$_\alpha$ (λ = 0.71073)
2Θ range for data collection/°	3.946 to 92.952
Index ranges	-15 ≤ h ≤ 15, -22 ≤ k ≤ 22, -26 ≤ l ≤ 26
Reflections collected	178231
Independent reflections	17847 [Rint = 0.0522, Rsigma = 0.0296]
Data/restraints/parameters	17847/1/264
Goodness-of-fit on F^2	1.019
Final R indexes [I>=2σ (I)]	R1 = 0.0291, wR2 =0.0485
Final R indexes [all data]	R1 = 0.0452, wR2 = 0.0525
Largest diff. peak/hole / e Å^{-3}	1.08/-1.10

Table S21 Bond Lengths for $Er(mpo)_3(H_2O)_2 \cdot H_2O$

Atom	Atom	Length/Å	Atom	Atom	Length/Å
Er1	S3	2.8413(4)	N3	C11	1.3665(19)
Er1	S2	2.7693(4)	N3	C15	1.355(2)
Er1	S1	2.7935(4)	N2	C6	1.3657(19)
Er1	O2	2.3327(10)	N2	C10	1.3519(19)
Er1	O1	2.3186(10)	C1	C2	1.409(2)
Er1	O4	2.3565(10)	C11	C12	1.413(2)
Er1	O3	2.3143(10)	C6	C7	1.405(2)
Er1	O5	2.3604(10)	C15	C14	1.366(3)
S3	C11	1.7042(16)	C5	C4	1.367(2)
S2	C6	1.7083(17)	C10	C9	1.369(2)
S1	C1	1.7060(16)	C2	C3	1.360(3)
O2	N2	1.3443(14)	C4	C3	1.390(3)
O1	N1	1.3452(15)	C12	C13	1.362(3)
O3	N3	1.3410(15)	C14	C13	1.385(4)
N1	C1	1.3674(18)	C9	C8	1.379(4)
N1	C5	1.3513(19)	C7	C8	1.361(3)

Table S22 Crystal data and structure refinement for $Tm(mpo)_3(H_2O)_2 \cdot H_2O$

Empirical formula	$C_{15}H_{18}N_3O_6S_3Tm$
Formula weight	601.43
Temperature/K	273.15
Crystal system	triclinic
Space group	$P\bar{1}$
a/Å	7.4398(9)
b/Å	11.1083(14)
c/Å	13.1269(16)
α/°	111.312(3)
β/°	94.019(3)
γ/°	91.182(3)
Volume/Å^3	1006.9(2)
Z	2
ρcalcg/cm^3	1.984
μ/mm^{-1}	4.754
F(000)	588.0
Crystal size/mm^3	0.539 × 0.24 × 0.171
Radiation	MoK$_\alpha$ (λ = 0.71073)
2Θ range for data collection/°	5.496 to 57.538
Index ranges	-10 ≤ h ≤ 10, -15 ≤ k ≤ 15, -17 ≤ l ≤ 17
Reflections collected	15505
Independent reflections	5179 [Rint = 0.0342, Rsigma = 0.0331]
Data/restraints/parameters	5179/0/258
Goodness-of-fit on F^2	1.184
Final R indexes [I>=2σ (I)]	R1 = 0.0232, wR2 =0.0560
Final R indexes [all data]	R1 = 0.0264, wR2 = 0.0587
Largest diff. peak/hole / e Å^{-3}	0.82/-1.03

Table S23 Bond Lengths for $Tm(mpo)_3(H_2O)_2 \cdot H_2O$

Atom	Atom	Length/Å	Atom	Atom	Length/Å
Tm1	S3	2.8371(9)	N1	C1	1.373(4)
Tm1	S1	2.7662(9)	N1	C5	1.359(4)
Tm1	S2	2.7854(9)	N2	C6	1.369(4)
Tm1	O1	2.325(2)	N2	C10	1.358(4)
Tm1	O2	2.312(2)	C1	C2	1.398(5)
Tm1	O5	2.349(2)	C11	C12	1.412(5)
Tm1	O3	2.306(2)	C6	C7	1.407(5)
Tm1	O4	2.353(2)	C15	C14	1.367(5)
S3	C11	1.704(4)	C5	C4	1.361(5)
S1	C1	1.709(4)	C10	C9	1.366(5)
S2	C6	1.711(4)	C14	C13	1.384(7)
O1	N1	1.346(3)	C7	C8	1.370(6)
O2	N2	1.350(3)	C2	C3	1.363(6)
O3	N3	1.343(3)	C12	C13	1.364(6)
N3	C11	1.371(4)	C9	C8	1.387(6)
N3	C15	1.356(4)	C4	C3	1.390(7)

Table S24 Crystal data and structure refinement for $Yb(mpo)_3(H_2O)_2 \cdot H_2O$

Empirical formula	$C_{15}H_{18}N_3O_6S_3Yb$
Formula weight	605.54
Temperature/K	296.15
Crystal system	triclinic
Space group	$P\bar{1}$
a/Å	7.4273(3)
b/Å	11.0844(4)
c/Å	13.0835(5)
α/°	111.299(2)
β/°	94.085(2)
γ/°	91.071(2)
Volume/Å^3	999.86(7)
Z	2
ρcalcg/cm^3	2.011
μ/mm^{-1}	5.027
F(000)	590.0
Crystal size/mm^3	0.243 × 0.2 × 0.188
Radiation	MoK$_\alpha$ (λ = 0.71073)
2Θ range for data collection/°	3.948 to 63.422
Index ranges	-10 ≤ h ≤ 10, -16 ≤ k ≤ 16, -19 ≤ l ≤ 19
Reflections collected	81495
Independent reflections	6745 [Rint = 0.0444, Rsigma = 0.0192]
Data/restraints/parameters	6745/0/272
Goodness-of-fit on F^2	1.101
Final R indexes [I>=2σ (I)]	R1 = 0.0204, wR2 =0.0499
Final R indexes [all data]	R1 = 0.0235, wR2 = 0.0511
Largest diff. peak/hole / e Å^{-3}	1.35/-0.88

Table S25 Bond Lengths for $Yb(mpo)_3(H_2O)_2 \cdot H_2O$

Atom	Atom	Length/Å	Atom	Atom	Length/Å
Yb1	S3	2.8301(7)	N1	C1	1.368(3)
Yb1	S2	2.7496(7)	N1	C5	1.354(3)
Yb1	S1	2.7714(7)	N2	C6	1.355(3)
Yb1	O2	2.3122(17)	N2	C10	1.357(4)
Yb1	O1	2.2967(18)	C11	C12	1.409(4)
Yb1	O4	2.3317(19)	C1	C2	1.414(4)
Yb1	O3	2.2953(18)	C5	C4	1.376(4)
Yb1	O5	2.341(2)	C6	C7	1.412(4)
S3	C11	1.703(3)	C10	C9	1.369(4)
S2	C6	1.708(3)	C15	C14	1.364(4)
S1	C1	1.705(3)	C14	C13	1.389(6)
O2	N2	1.350(3)	C2	C3	1.358(5)
O1	N1	1.349(3)	C4	C3	1.381(5)
O3	N3	1.336(3)	C12	C13	1.361(5)
N3	C11	1.371(3)	C9	C8	1.377(6)
N3	C15	1.355(3)	C8	C7	1.360(5)

Table S26 Crystal data and structure refinement for $Lu(mpo)_3(H_2O)_2 \cdot H_2O$

Empirical formula	$C_{15}H_{19}LuN_3O_6S_3$
Formula weight	608.48
Temperature/K	273.15
Crystal system	triclinic
Space group	$P\bar{1}$
a/Å	7.4092(3)
b/Å	11.0676(5)
c/Å	13.0778(6)
α/°	111.325(2)
β/°	94.072(2)
γ/°	91.141(2)
Volume/Å^3	995.25(8)
Z	2
ρcalcg/cm^3	2.030
μ/mm^{-1}	5.312
F(000)	594.0
Crystal size/mm^3	0.465 × 0.248 × 0.166
Radiation	MoK$_\alpha$ (λ = 0.71073)
2Θ range for data collection/°	5.518 to 55.124
Index ranges	-9 ≤ h ≤ 9, -14 ≤ k ≤ 14, -16 ≤ l ≤ 16
Reflections collected	72598
Independent reflections	4577 [Rint = 0.0548, Rsigma = 0.0190]
Data/restraints/parameters	4577/1/264
Goodness-of-fit on F^2	1.086
Final R indexes [I>=2σ (I)]	R1 = 0.0167, wR2 =0.0393
Final R indexes [all data]	R1 = 0.0194, wR2 = 0.0408
Largest diff. peak/hole / e Å^{-3}	0.91/-0.66

Table S27 Bond Lengths for $Lu(mpo)_3(H_2O)_2 \cdot H_2O$

Atom	Atom	Length/Å	Atom	Atom	Length/Å
Lu1	S3	2.8224(7)	N2	C10	1.345(3)
Lu1	S1	2.7405(7)	N2	C6	1.369(3)
Lu1	S2	2.7611(7)	N1	C1	1.365(3)
Lu1	O2	2.2920(18)	N1	C5	1.354(3)
Lu1	O1	2.3029(16)	C11	C12	1.404(4)
Lu1	O4	2.3206(17)	C10	C9	1.370(4)
Lu1	O3	2.2888(17)	C15	C14	1.363(4)
Lu1	O5	2.3243(18)	C1	C2	1.405(4)
S3	C11	1.702(3)	C6	C7	1.406(4)
S1	C1	1.706(3)	C5	C4	1.362(4)
S2	C6	1.704(3)	C14	C13	1.383(5)
O2	N2	1.347(3)	C12	C13	1.356(5)
O1	N1	1.344(2)	C9	C8	1.384(5)
O3	N3	1.340(3)	C7	C8	1.368(5)
N3	C11	1.369(3)	C2	C3	1.357(5)
N3	C15	1.354(3)	C4	C3	1.378(6)

Table S28 Crystal data and structure refinement for $[Am(mpo)_2(\mu\text{-O-mpo})(H_2O)]_2 \cdot 3H_2O$	
Empirical formula	$C_{15}H_{20}AmN_3O_7S_3$
Formula weight	693.52
Temperature/K	100.15
Crystal system	triclinic
Space group	$P\bar{1}$
a/Å	8.3942(10)
b/Å	9.6982(10)
c/Å	13.6896(18)
α/°	92.332(5)
β/°	107.744(4)
γ/°	92.932(3)
Volume/Å^3	1058.2(2)
Z	2
ρcalcg/cm^3	2.177
μ/mm^{-1}	3.963
F(000)	660.0
Crystal size/mm^3	0.536 × 0.298 × 0.19
Radiation	MoK$_\alpha$ (λ = 0.71073)
2Θ range for data collection/°	5.104 to 56.706
Index ranges	$-11 \leq h \leq 11$, $-12 \leq k \leq 12$, $-18 \leq l \leq 18$
Reflections collected	54347
Independent reflections	5265 [Rint = 0.0711, Rsigma = 0.0311]
Data/restraints/parameters	5265/1/274
Goodness-of-fit on F^2	1.178
Final R indexes [I>=2σ (I)]	R1 = 0.0392, wR2 =0.0960
Final R indexes [all data]	R1 = 0.0406, wR2 = 0.0973
Largest diff. peak/hole / e Å^{-3}	2.87/-4.89

Table S29 Bond Lengths for $[Am(mpo)_2(\mu\text{-O-mpo})(H_2O)]_2 \cdot 3H_2O$					
Atom	**Atom**	**Length/Å**	**Atom**	**Atom**	**Length/Å**
Am1	S2	2.8890(16)	N1	C5	1.352(8)
Am1	S3	2.8734(16)	N1	C1	1.371(8)
Am1	S1	2.9453(16)	N2	C6	1.353(8)
Am1	O11	2.519(4)	N2	C10	1.360(8)
Am1	O1	2.468(4)	N3	C15	1.357(9)
Am1	O3	2.355(5)	N3	C11	1.358(8)
Am1	O2	2.366(4)	C5	C4	1.361(9)
Am1	N1	3.254(5)	C6	C7	1.409(9)
Am1	N11	3.439(5)	C7	C8	1.380(9)
Am1	O4	2.441(5)	C15	C14	1.379(9)
Am1	N2	3.401(5)	C11	C12	1.414(9)
Am1	N3	3.391(5)	C8	C9	1.398(10)
S2	C6	1.721(6)	C4	C3	1.396(12)
S3	C11	1.713(7)	C9	C10	1.357(10)
S1	C1	1.730(7)	C14	C13	1.394(10)
O1	N1	1.349(6)	C12	C13	1.376(10)
O3	N3	1.337(6)	C1	C2	1.414(9)
O2	N2	1.358(7)	C2	C3	1.362(12)

[1]1-X,1-Y,1-Z

^{1}H Nuclear Magnetic Resonance Spectroscopy

^{1}H NMR spectra of **1-Ln** (Pr, Sm, Nd, Eu) and **2-Ln** (Yb, Lu) were collected in pyridine-d_5 as other solvents quickly precipitated the solids, see below. Spectra of **1-Ln** reveals four resonances that correspond with the four distinct resonances present in the major thiol form of pyrithione. Both **1-Pr** and **1-Nd** show paramagnetic broadening typical of both $4f^2$ and $4f^3$ systems ranging from 31 to 21 ppm, respectively. The spectrum of **1-Sm** exhibits peak splitting that is also observable in spectra of the free ligand: two triplets of doublets at 7.11 and 7.22 ppm correspond to aromatic protons meta- to the sulfur and N-oxide groups while the two doublets at 8.00 and 9.79 ppm are assigned to the protons meta- to these chelating moieties. Similarly, spectra of **1-Eu** and **2-Yb** show four, paramagnetically broadened resonances that are shifted upfield at -5.37 and -35.20 ppm, respectively. Paramagnetic shifting of the other **1-Ln** (Gd, Tb) and **2-Ln** (Dy, Ho, Er, Tm) complexes was significant such that no set of resonances are observable. Due to sample constraints and radioactive hazards, ^{1}H NMR was unable to be collected on **1-Am**.

Monomeric **2-Ln** contains three symmetric pyrithionate ligands which yield a single set of resonances, **Figures S17** and **S18**. A single set of resonances is observed in **1-Ln**, which indicates either a dynamic process via monomer-dimer equilibrium or dissociation of the dimers in the solution-state. Future studies using this ligand should investigate the behavior of **2-Ln** in the solution-state using other deuterated, less complexing solvents.

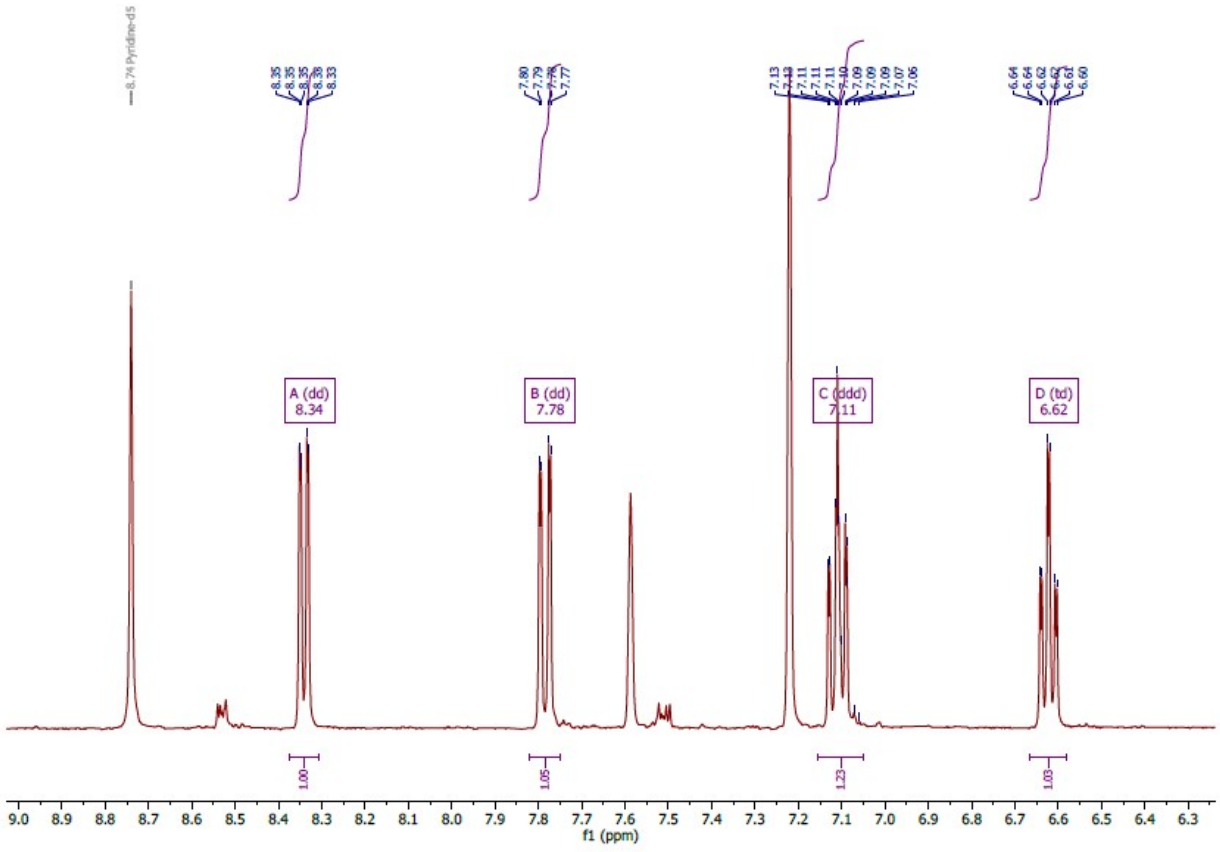

Figure S14: Pyrithione, free ligand

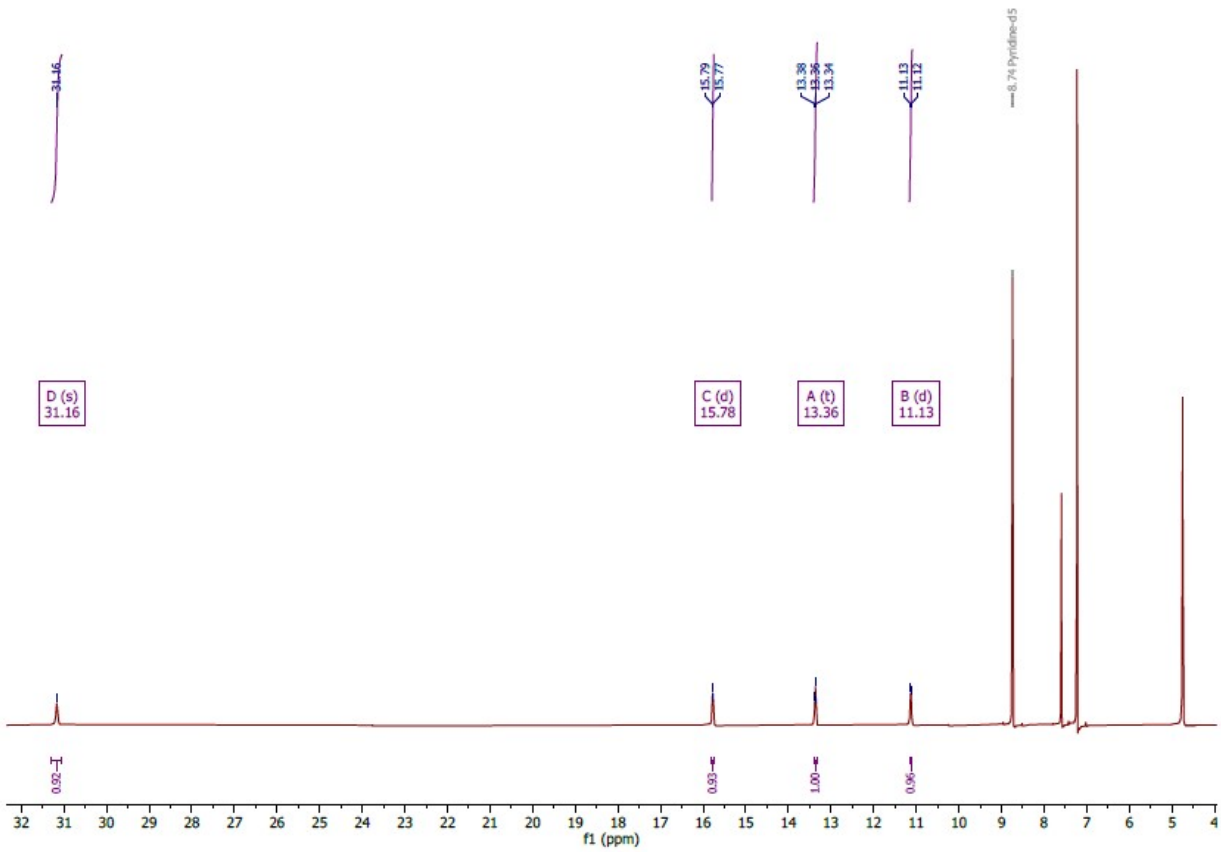

Figure S15: $[Pr(mpo)_2(\mu\text{-O-mpo})(H_2O)]_2$

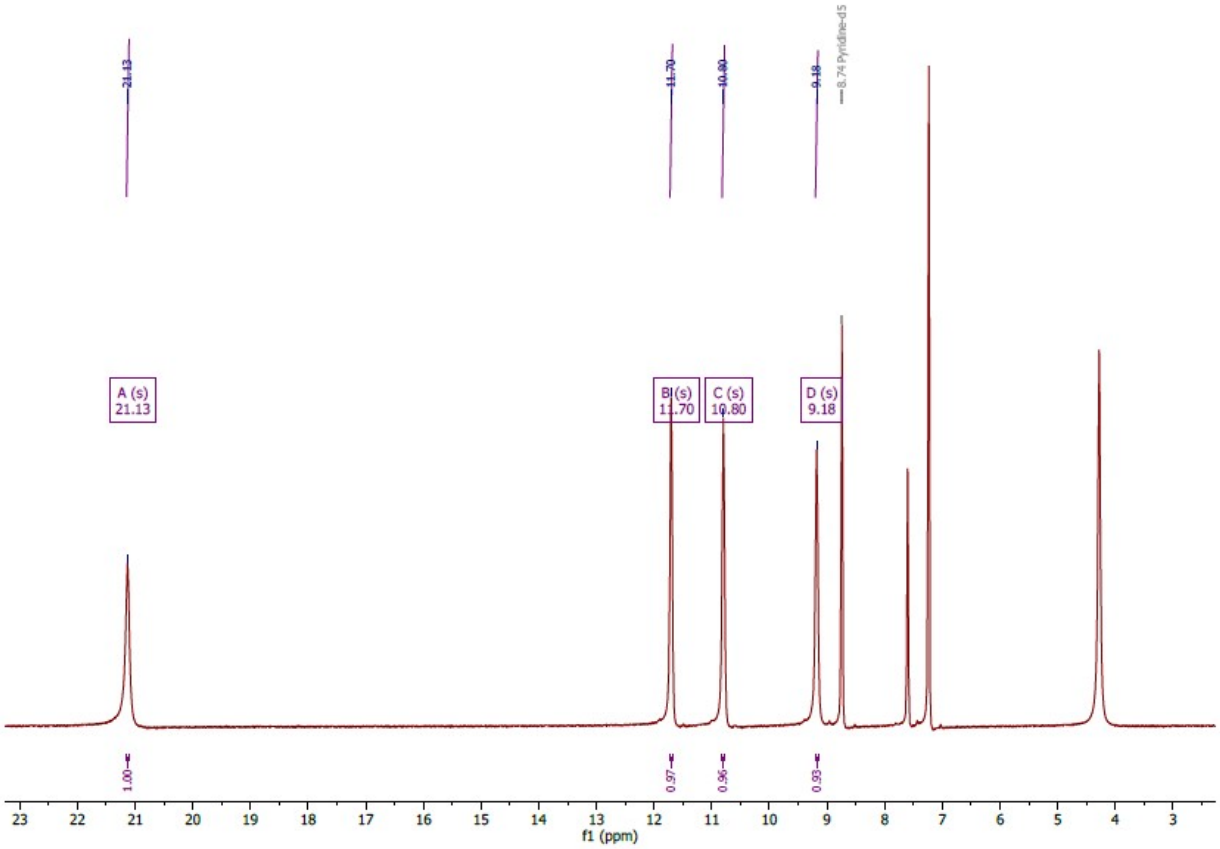

Figure S16: $[Nd(mpo)_2(\mu\text{-O-mpo})(H_2O)]_2$

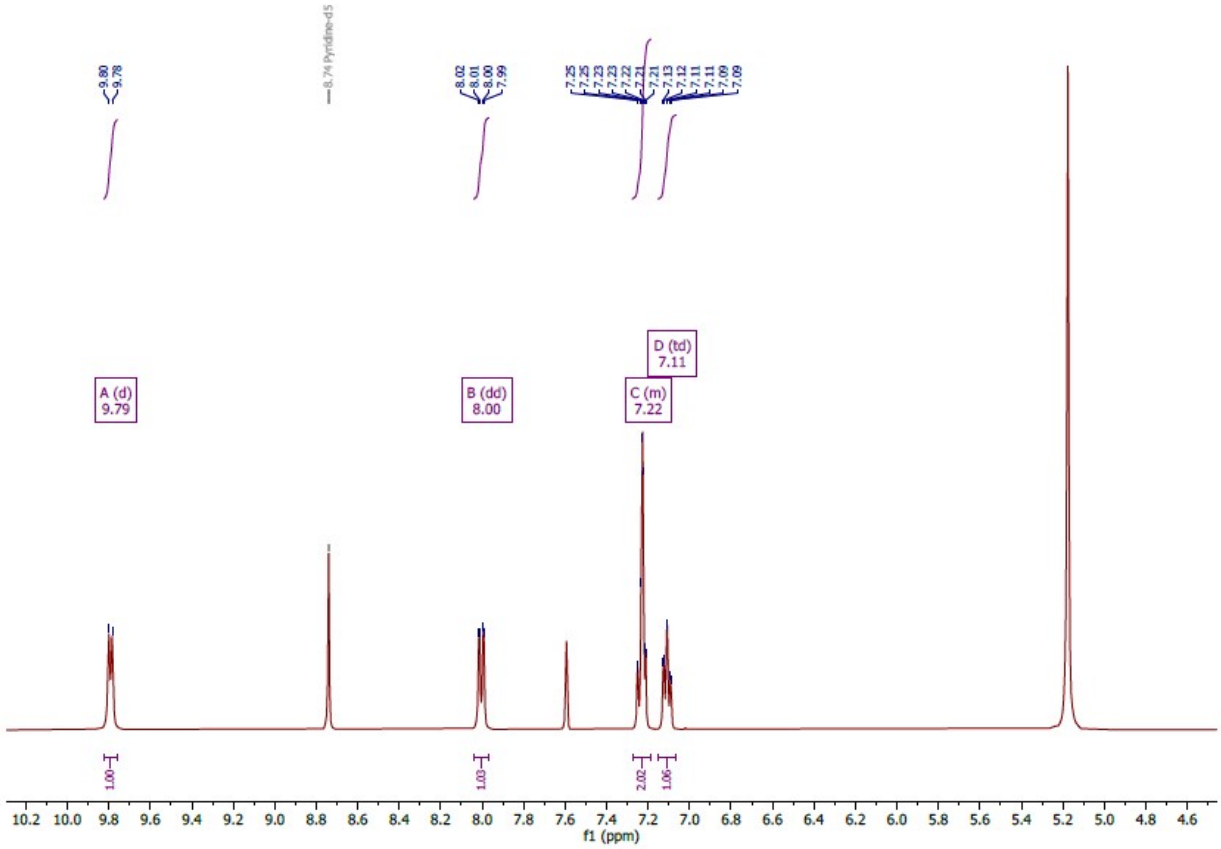

Figure S17: $[Sm(mpo)_2(\mu\text{-O-mpo})(H_2O)]_2$

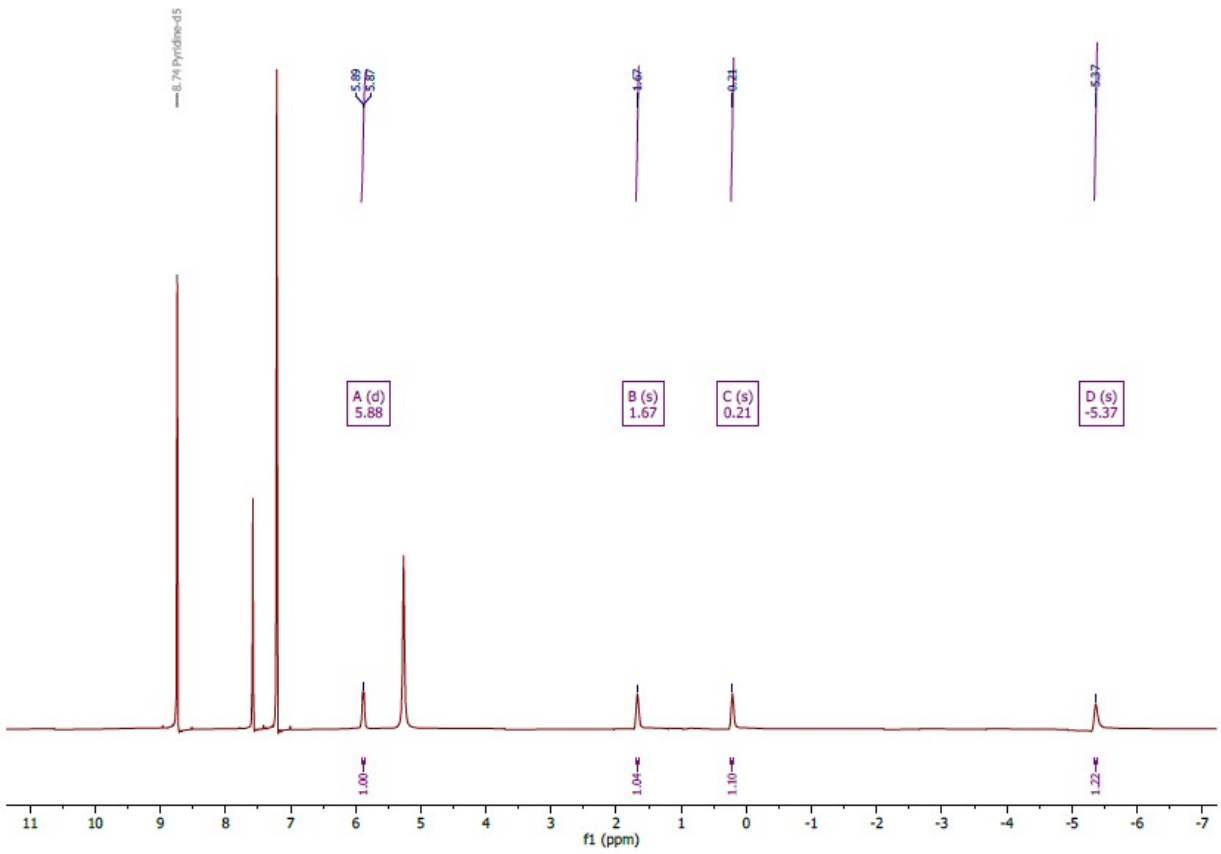

Figure S18: $[Eu(mpo)_2(\mu\text{-O-mpo})(H_2O)]_2$

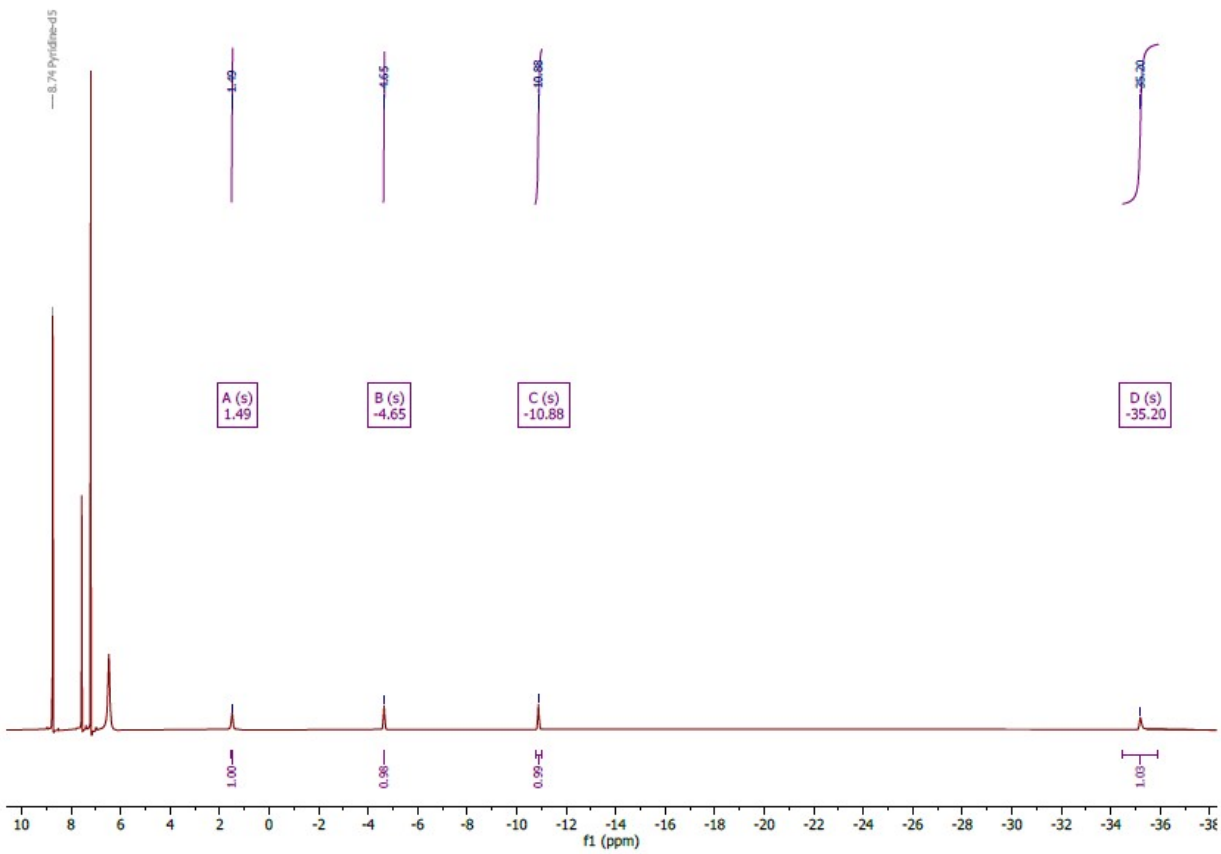

Figure S19: $Yb(mpo)_3(H_2O)_2 \bullet H_2O$

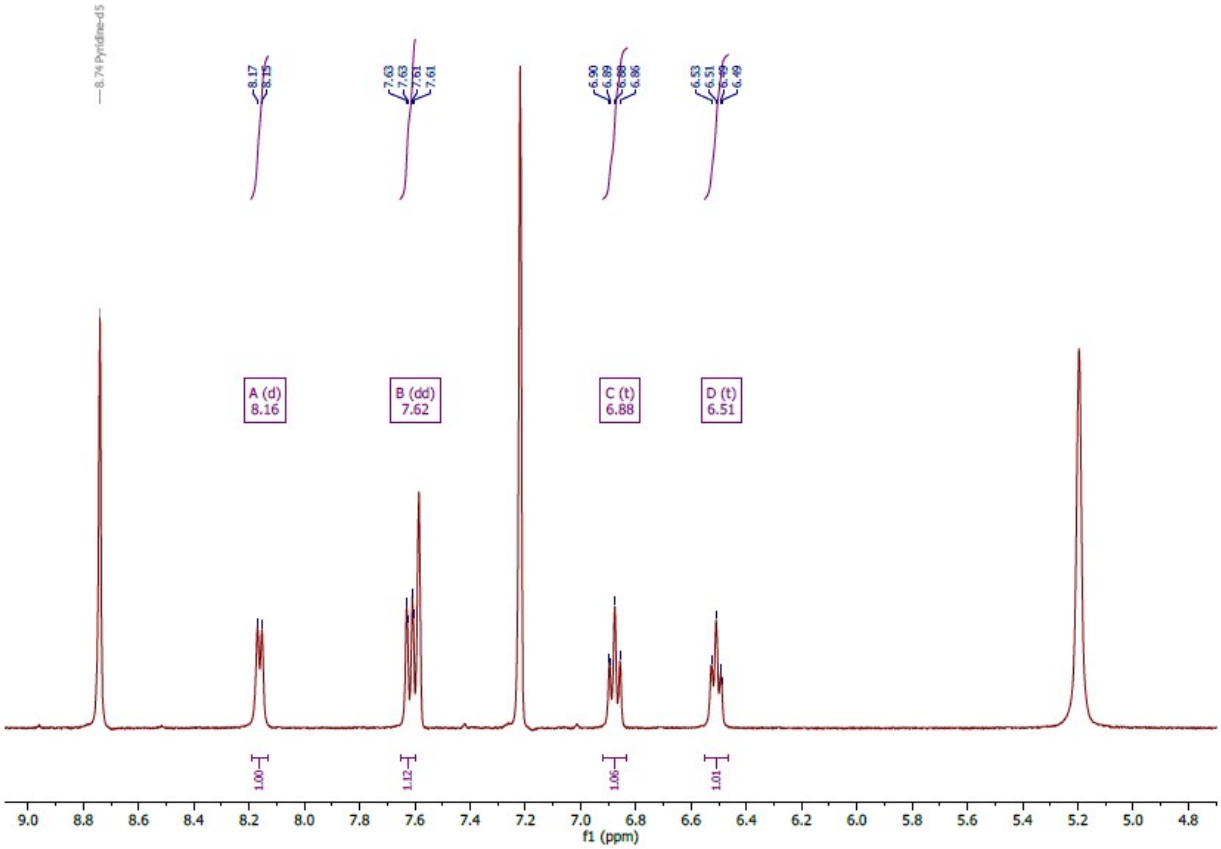

Figure S20: $Lu(mpo)_3(H_2O)_2 \cdot H_2O$

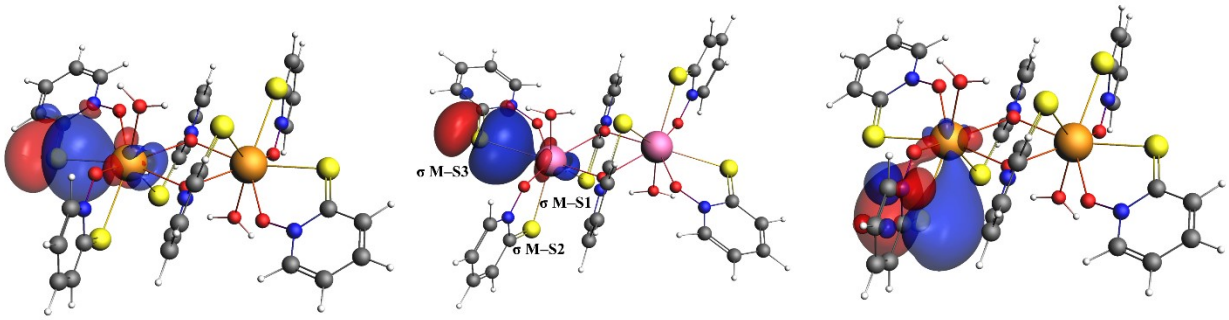

σ M–S1	Not observed in Am Not observed in Nd Not observed in Eu	σ M–S1	(0.16) 2% Am (0.10 7s : 0.70 6d : 0.20 5f) (0.13) 3% Nd (0.78 5d : 0.21 4f) (0.12) 6% Eu (0.21 6s : 0.74 5d : 0.05 4f)	π M–S1	Not observed in Am Not observed in Nd Not observed in Eu
σ M–S2	Not observed in Am Not observed in Nd Not observed in Eu	σ M–S2	(0.19) 8% Am (0.24 7s : 0.68 6d : 0.08 5f) (0.18) 8% Nd (0.17 6s : 0.69 5d : 0.14 4f) (0.16) 8% Eu (0.28 6s : 0.62 5d : 0.09 4f)	π M–S2	(0.13) 7% Am (0.38 6d : 0.62 5f) Not observed in Nd Not observed in Eu
σ M–S3	(0.31) 15% Am (0.16 7s : 0.42 6d : 0.42 5f) Not observed in Nd Not observed in Eu	σ M–S3	(0.04) 10% Am (0.21 7s : 0.78 6d) (0.18) 9% Nd (0.22 6s : 0.56 5d : 0.22 4f) (0.18) 9% Eu (0.24 6s : 0.54 5d : 0.21 4f)	π M–S3	Not observed in Am Not observed in Nd Not observed in Eu

Figure S21. Selected natural localized molecular orbitals (NLMOs) showing the main metal – sulfur interactions. Metal contributions to the NLMOs are shown along with their hybrid contributions and contribution to the NLMO-BI (brackets).

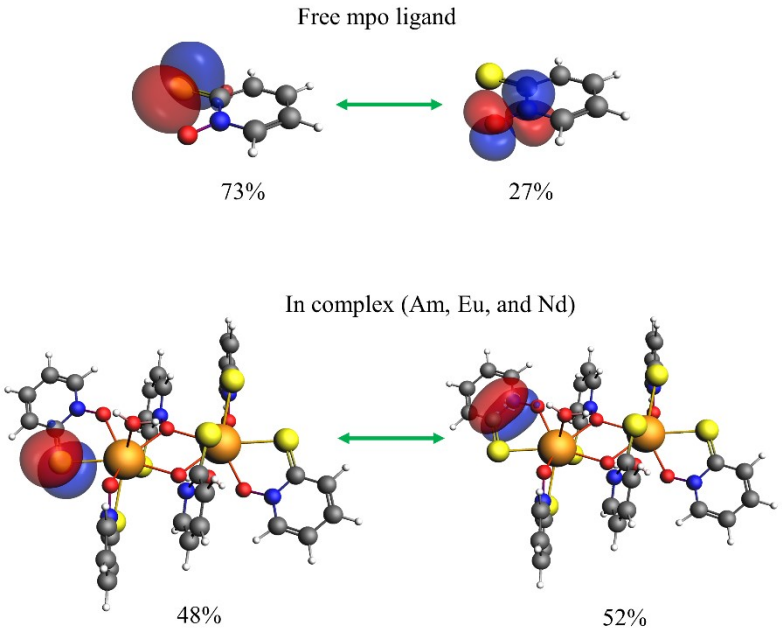

Figure S22. Selected hyperbonds (3-center 4-electron bonds) observed in the free mpo ligand and in complexes **1-Am, 1-Eu,** and **1-Nd**. The orbitals shown correspond to the natural bond orbitals (NBOs) involved in hyperbonding (A: + B–C → A–B + :C).

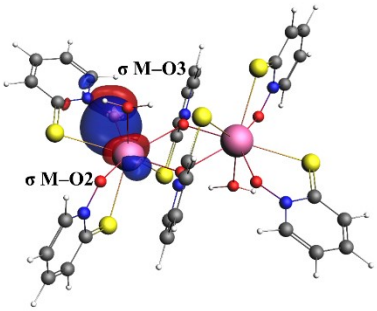

σ M–O2	(0.14) 7% Am (0.13 7s : 0.63 6d : 0.24 5f) (0.10) 5% Nd (0.12 6s : 0.65 5d : 0.24 4f) (0.08) 4% Eu (0.16 6s : 0.82 5d : 0.02 4f)
σ M–O3	(0.12) 6% Am (0.16 7s : 0.79 6d : 0.05 5f) (0.10) 5% Nd (0.11 6s : 0.66 5d : 0.24 4f) (0.10) 5% Eu (0.15 6s : 0.70 5d : 0.15 4f)

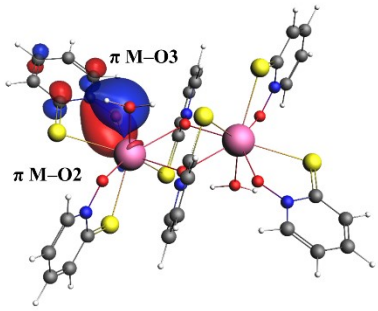

π M–O2	(0.08) 4% Am (0.50 6d : 0.50 5f) (0.05) 3% Nd (0.71 5d : 0.29 4f) (0.04) 2% Eu (0.69 5d : 0.31 4f)
π M–O3	(0.05) 4% Am (0.93 6d : 0.07 5f) (0.05) 3% Nd (0.56 5d : 0.44 4f) (0.04) 2% Eu (0.98 5d : 0.02 4f)

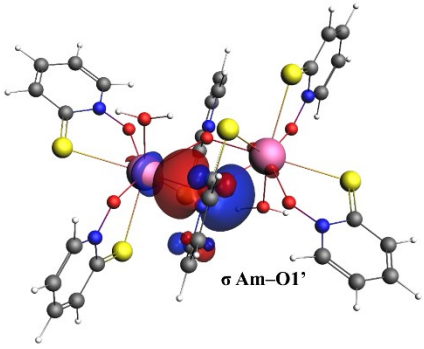

σ M–O1'	(0.09) 4% Am (0.08 7s : 0.49 6d : 0.43 5f) (0.06) 3% Nd (0.17 6s : 0.71 5d : 0.11 4f) (0.02) 2% Eu (0.13 6s : 0.86 5d : 0.01 4f)

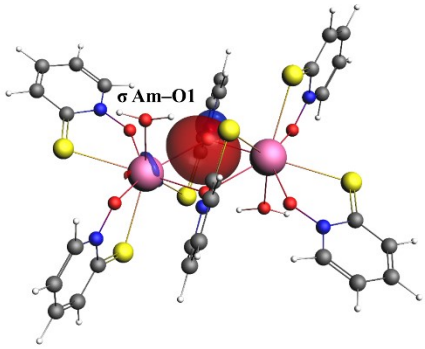

σ M–O1	(0.03) 3% Am (0.14 7s : 0.74 6d : 0.12 5f) (0.02) 2% Nd (0.06 6s : 0.58 5d : 0.35 4f) (0.03) 2% Eu (0.22 6s : 0.77 5d : 0.01 4f)

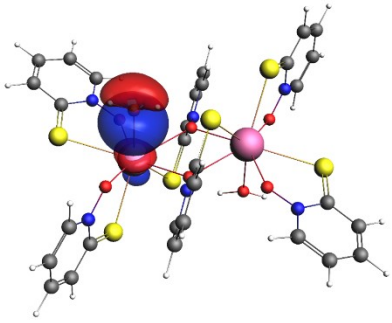

σ M–OH_2	(0.08) 4% Am (0.21 7s : 0.75 6d : 0.04 5f) (0.06) 5% Nd (0.20 6s : 0.70 5d : 0.11 4f) (0.06) 3% Eu (0.25 6s : 0.74 5d : 0.01 4f)

Figure S23. Selected natural localized molecular orbitals (NLMOs) showing the main metal – oxygen interactions. Metal contributions to the NLMOs are shown along with their hybrid contributions and contribution to the NLMO-BI (brackets).

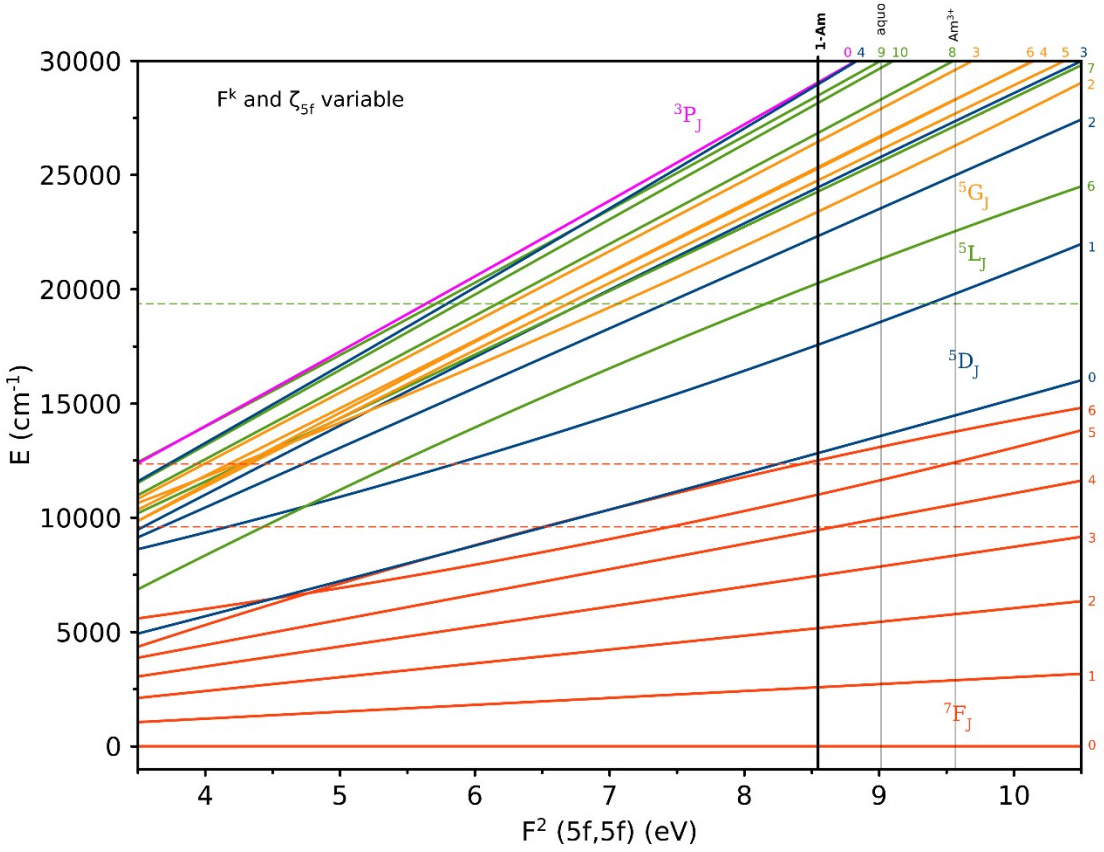

Figure S24. LFDFT energy levels of Am(III) as a function of F^k and ζ_{5f} parameters. It was assumed that F^4, F^6, and ζ_{5f} are dependent functions of F^2. The vertical black line refers to the position of the electronic structure of **1-Am**, while grey vertical lines are shown as references for a nona-aquo and free Am^{3+} ions. For simplicity the Russell-Saunders notation has been used to label the nature of the ground and excited states.

Table S30. Wiberg (WBI) and Natural Localized Molecular Orbital bond indices (NLMO-BI). Labels correspond to the **1-Am** structure in **Figure 3**.

	WBI			NLMO-BI		
M - L bond*	**1-Nd**	**1-Eu**	**1-Am**	**1-Nd**	**1-Eu**	**1-Am**
S1	0.333	0.313	0.393	0.219	0.198	0.251
S2	0.461	0.419	0.501	0.306	0.264	0.348
S3	0.451	0.413	0.568	0.296	0.253	0.433
O1	0.183	0.153	0.245	0.099	0.085	0.131
O2	0.318	0.257	0.386	0.176	0.143	0.218
O3	0.316	0.262	0.382	0.173	0.150	0.202
O1’	0.185	0.154	0.248	0.105	0.086	0.147
OH_2	0.186	0.163	0.226	0.090	0.080	0.101

Table S31. Selected mpo bond lengths of the free and in-complex geometries. The free mpo bond lengths correspond to those obtained by geometry optimization at the PBE/TZP level of theory.

Bond	System	Average distance
	1-Am	1.723
C–S	**1-Nd**	1.711
	Free mpo	1.705
	1-Am	1.360
C–N	**1-Nd**	1.360
	Free mpo	1.440
	1-Am	1.347
N–O	**1-Nd**	1.333
	Free mpo	1.294

Table S32. Wiberg bond indices of the free and in-complex mpo. WBIs of complexed mpo correspond to average values of all coordinated mpo ligands.

WBI	mpo	**1-Nd**	**1-Am**	$\Delta WBI_{mpo\text{-}1\text{-}Am}$	$\Delta WBI_{1\text{-}Nd\text{-}1\text{-}Am}$
C-S	1.394	1.276	1.273	0.121	0.002
C-N	1.036	1.151	1.154	-0.118	-0.003
N-O	1.274	1.107	1.101	0.173	0.007

Table S33. Average wavefunction composition of the low-lying states of **1-Am** calculated from LFDFT. Contributions < 5% were omitted.

Relative energy (cm^{-1})	J	Wavefunction composition
0	0	50% ^{7}F + 36% ^{5}D + 12% ^{3}P
2,467 – 2,800	1	68% ^{7}F + 27% ^{5}D
5,064 – 5,517	2	81% ^{7}F + 15% ^{5}D
7,411 – 7,745	3	86% ^{7}F + 6% ^{5}D
9,100 – 9,926	4	87% ^{7}F + 5% ^{5}D
10,827 – 11,570	5	82% ^{7}F + 10% ^{5}G + 5% ^{5}F
11,944 – 12,590	6	72% ^{7}F + 21% ^{5}G

"Pr"

SAMPLE IDENTIFICATION ON Vial

Analysis Requested: CHN

Single ☐ Duplicate ☑ Triplicate ☐

Analysis Requested	Customer Theory	*Office Use Only: Results are total % Found*		
C	33.3%	32.98	33.01	
H	3.1%	2.63	2.69	
N	7.8%	7.60	7.59	

Molecular Formula:	Pr(C5H5NOS)3(H2O)
Air Sensitive/ Glove Box:	YES ☐ NO ☑
Hazardous/ Explosive:	YES ☐ NO ☑
Hydroscopic:	YES ☐ NO ☑
Vacuum Drying Requested: Yes ☐ No ☑	Temp: _____ °C Time: ____ Hr. ____ Min.
Sample Return Address: Yes ☐ No ☑	

Shipping address:
Midwest Microlab
Attn: Valerie Guzzetta
7212 N. Shadeland Ave., Suite 110
Indianapolis, IN 46250
Phone: 317-849-6606
Fax: 317-849-8534
Email: info@midwestlab.com
Website: www.midwestlab.com

Submitter Comments:

Office Use Only

Please include 1 submission form per sample.

RECEIVED AUG 22 2022

We appreciate your business.

Figure S25: CHN Analysis of **1-Pr**.

"Nd"

SAMPLE IDENTIFICATION ON Vial

Analysis Requested: CHN

Single ☐ Duplicate ☑ Triplicate ☐

Analysis Requested	Customer Theory	*Office Use Only: Results are total % Found*		
C	33.1%	33.48	33.35	
H	3.1%	2.57	2.27	
N	7.7%	7.69	7.32	

Molecular Formula:	Nd(C5H5NOS)3(H2O)
Air Sensitive/ Glove Box:	YES ☐ NO ☑
Hazardous/ Explosive:	YES ☐ NO ☑
Hydroscopic:	YES ☐ NO ☑
Vacuum Drying Requested: Yes ☐ No ☑	Temp: _____ °C Time: ____ Hr. ____ Min.
Sample Return Address: Yes ☐ No ☑	

Shipping address:
Midwest Microlab
Attn: Valerie Guzzetta
7212 N. Shadeland Ave., Suite 110
Indianapolis, IN 46250
Phone: 317-849-6606
Fax: 317-849-8534
Email: info@midwestlab.com
Website: www.midwestlab.com

Submitter Comments:

Office Use Only

Please include 1 submission form per sample.

We appreciate your business.

RECEIVED AUG 2 2 2022

Figure S26: CHN Analysis of **1-Nd**.

MIDWESTMICRO lab

"Sm"

SAMPLE IDENTIFICATION ON Vial

Analysis Requested: CHN

Single ☐ Duplicate ☑ Triplicate ☐

Analysis Requested	Customer Theory	*Office Use Only: Results are total % Found*		
C	32.7%	32.85	33.05	
H	3.1%	2.53	2.59	
N	7.6%	7.54	7.54	

Molecular Formula:	Sm(C5H5NOS)3 (H2O)
Air Sensitive/ Glove Box:	YES ☐ NO ☑
Hazardous/ Explosive:	YES ☐ NO ☑
Hydroscopic:	YES ☐ NO ☑
Vacuum Drying Requested: Yes ☐ No ☑	Temp: _____ °C Time: ___ Hr. ___ Min.
Sample Return Address: Yes ☐ No ☑	

Shipping address:
Midwest Microlab
Attn: Valerie Guzzetta
7212 N. Shadeland Ave., Suite 110
Indianapolis, IN 46250
Phone: 317-849-6606
Fax: 317-849-8534
Email: info@midwestlab.com
Website: www.midwestlab.com

Submitter Comments:

Office Use Only

Please include 1 submission form per sample.

RECEIVED AUG 22 2022

We appreciate your business.

Figure S27: CHN Analysis of **1-Sm**.

"Eu"

SAMPLE IDENTIFICATION ON Vial

Analysis Requested: CHN

Single ☐ Duplicate ☑ Triplicate ☐

Analysis Requested	Customer Theory	*Office Use Only: Results are total % Found*		
C	32.7%	35.39	**	
H	3.1%	3.09		
N	7.6%	7.94		

Molecular Formula:	Eu(C5H5NOS)3(H2O)
Air Sensitive/ Glove Box:	YES ☐ NO ☑
Hazardous/ Explosive:	YES ☐ NO ☑
Hydroscopic:	YES ☐ NO ☑
Vacuum Drying Requested: Yes ☐ No ☑	Temp: _____ °C Time: ____ Hr. ____ Min.
Sample Return Address: Yes ☐ No ☑	

Shipping address:
Midwest Microlab
Attn: Valerie Guzzetta
7212 N. Shadeland Ave., Suite 110
Indianapolis, IN 46250
Phone: 317-849-6606
Fax: 317-849-8534
Email: info@midwestlab.com
Website: www.midwestlab.com

Submitter Comments:

Office Use Only

** Sample lid was not screwed on and the sample leaked all over. Only 0.794 mg of sample was viable in the vial.**

Please include 1 submission form per sample.

RECEIVED AUG 22 2022

We appreciate your business.

Figure S28: CHN Analysis of **1-Eu**.

MIDWESTMICRO lab

"Gd"

SAMPLE IDENTIFICATION ON Vial

Analysis Requested: CHN

Single ☐ Duplicate ☑ Triplicate ☐

Analysis Requested	Customer Theory	*Office Use Only: Results are total % Found*		
C	32.3%	31.70	31.66	
H	3.1%	2.56	2.74	
N	7.5%	7.25	6.96	

Molecular Formula:	Gd(C5H5NOS)3 (H2O)
Air Sensitive/ Glove Box:	YES ☐ NO ☑
Hazardous/ Explosive:	YES ☐ NO ☑
Hydroscopic:	YES ☐ NO ☑
Vacuum Drying Requested: Yes ☐ No ☑	Temp: _____ °C Time: ____ Hr. ____ Min.
Sample Return Address: Yes ☐ No ☑	

Shipping address:
Midwest Microlab
Attn: Valerie Guzzetta
7212 N. Shadeland Ave., Suite 110
Indianapolis, IN 46250
Phone: 317-849-6606
Fax: 317-849-8534
Email: info@midwestlab.com
Website: www.midwestlab.com

Submitter Comments:

Office Use Only

Please include 1 submission form per sample.

RECEIVED AUG 22 2022

We appreciate your business.

Figure S29: CHN Analysis of **1-Gd**.

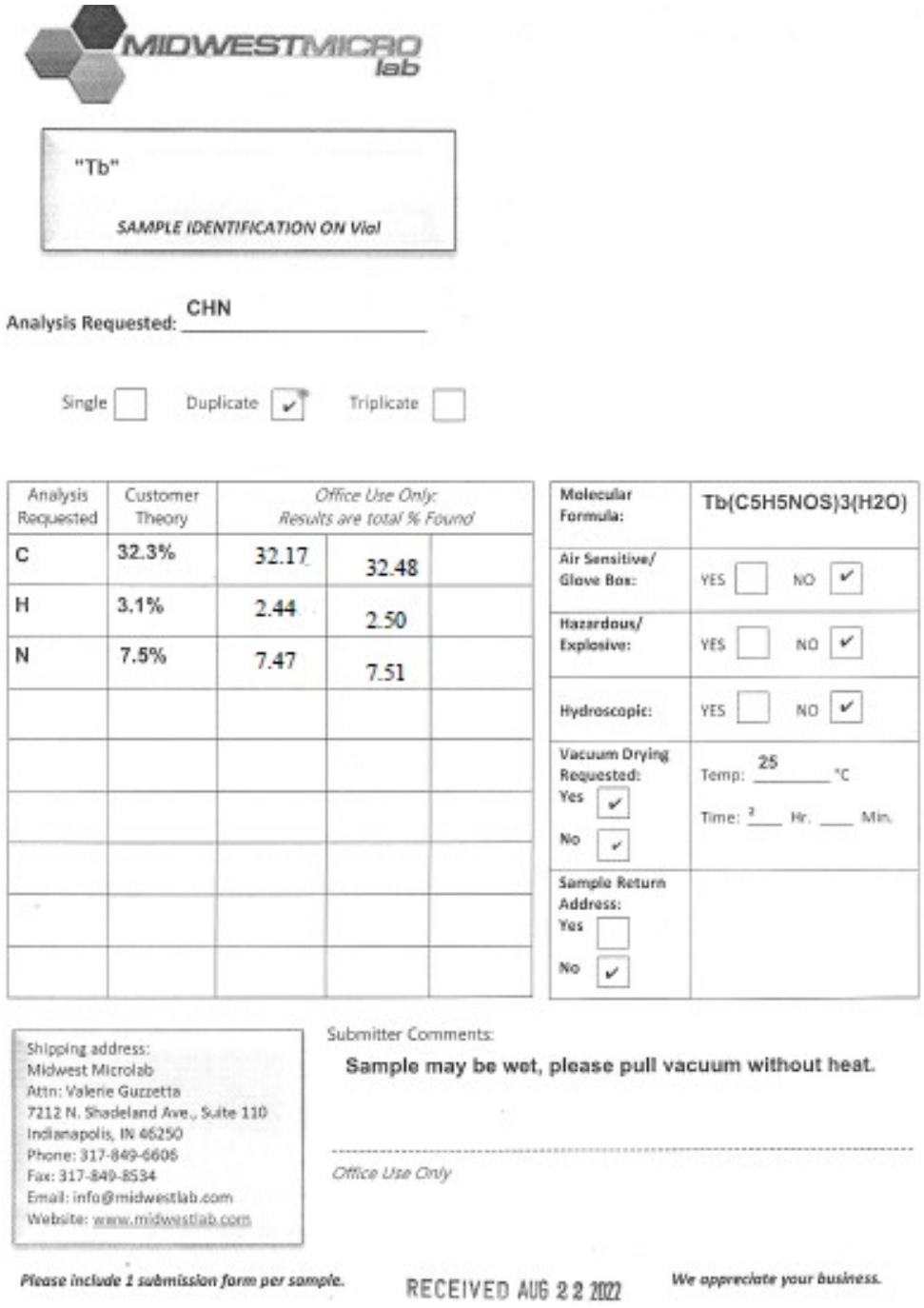

MIDWESTMICRO lab

"Tb"

SAMPLE IDENTIFICATION ON Vial

Analysis Requested: CHN

Single ☐ Duplicate ☑ Triplicate ☐

Analysis Requested	Customer Theory	*Office Use Only: Results are total % Found*		
C	32.3%	32.17	32.48	
H	3.1%	2.44	2.50	
N	7.5%	7.47	7.51	

Molecular Formula:	Tb(C5H5NOS)3(H2O)
Air Sensitive/ Glove Box:	YES ☐ NO ☑
Hazardous/ Explosive:	YES ☐ NO ☑
Hydroscopic:	YES ☐ NO ☑
Vacuum Drying Requested: Yes ☑ No ☑	Temp: 25 °C Time: 3 Hr. ___ Min.
Sample Return Address: Yes ☐ No ☑	

Shipping address:
Midwest Microlab
Attn: Valerie Guzzetta
7212 N. Shadeland Ave., Suite 110
Indianapolis, IN 46250
Phone: 317-849-6606
Fax: 317-849-8534
Email: info@midwestlab.com
Website: www.midwestlab.com

Submitter Comments:
Sample may be wet, please pull vacuum without heat.

Office Use Only

Please include 1 submission form per sample.

RECEIVED AUG 2 2 2022

We appreciate your business.

Figure S30: CHN Analysis of **1-Tb**.

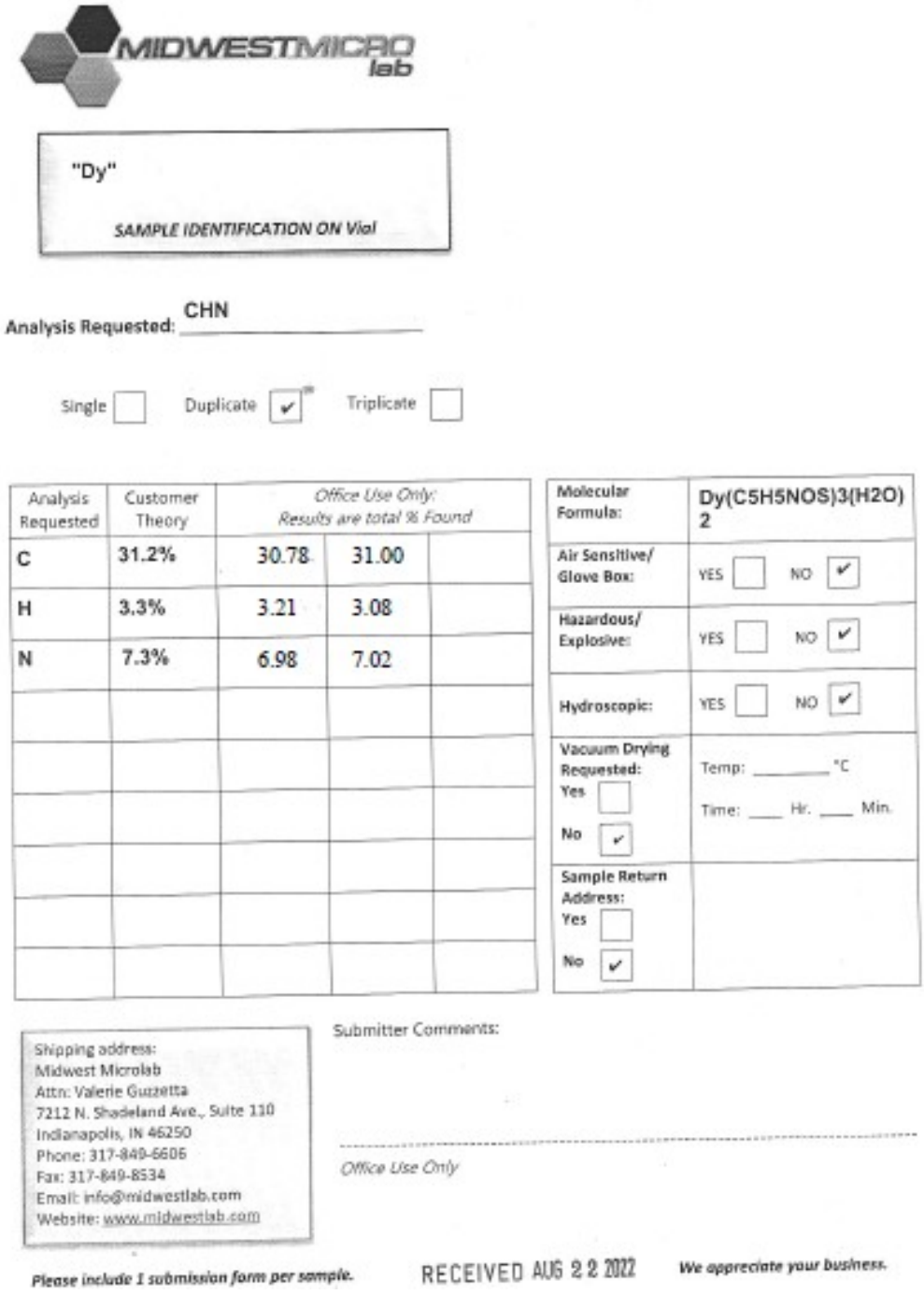

Figure S31: CHN Analysis of **2-Dy**.

"Ho"

SAMPLE IDENTIFICATION ON Vial

Analysis Requested: CHN

Single ☐ Duplicate ☑ Triplicate ☐

Analysis Requested	Customer Theory	*Office Use Only: Results are total % Found*		
C	30.1%	30.14	30.99	
H	3.3%	2.92	3.29	
N	7.2%	6.92	6.76	

Molecular Formula:	Ho(C5H5NOS)3(H2O)2
Air Sensitive/ Glove Box:	YES ☐ NO ☑
Hazardous/ Explosive:	YES ☐ NO ☑
Hydroscopic:	YES ☐ NO ☑
Vacuum Drying Requested: Yes ☐ No ☑	Temp: _____ °C Time: ___ Hr. ___ Min.
Sample Return Address: Yes ☐ No ☑	

Shipping address:
Midwest Microlab
Attn: Valerie Guzzetta
7212 N. Shadeland Ave., Suite 110
Indianapolis, IN 46250
Phone: 317-849-6606
Fax: 317-849-8534
Email: info@midwestlab.com
Website: www.midwestlab.com

Submitter Comments:

Office Use Only

Please include 1 submission form per sample.

RECEIVED AUG 2 2 2022

We appreciate your business.

Figure S32: CHN Analysis of **2-Ho**.

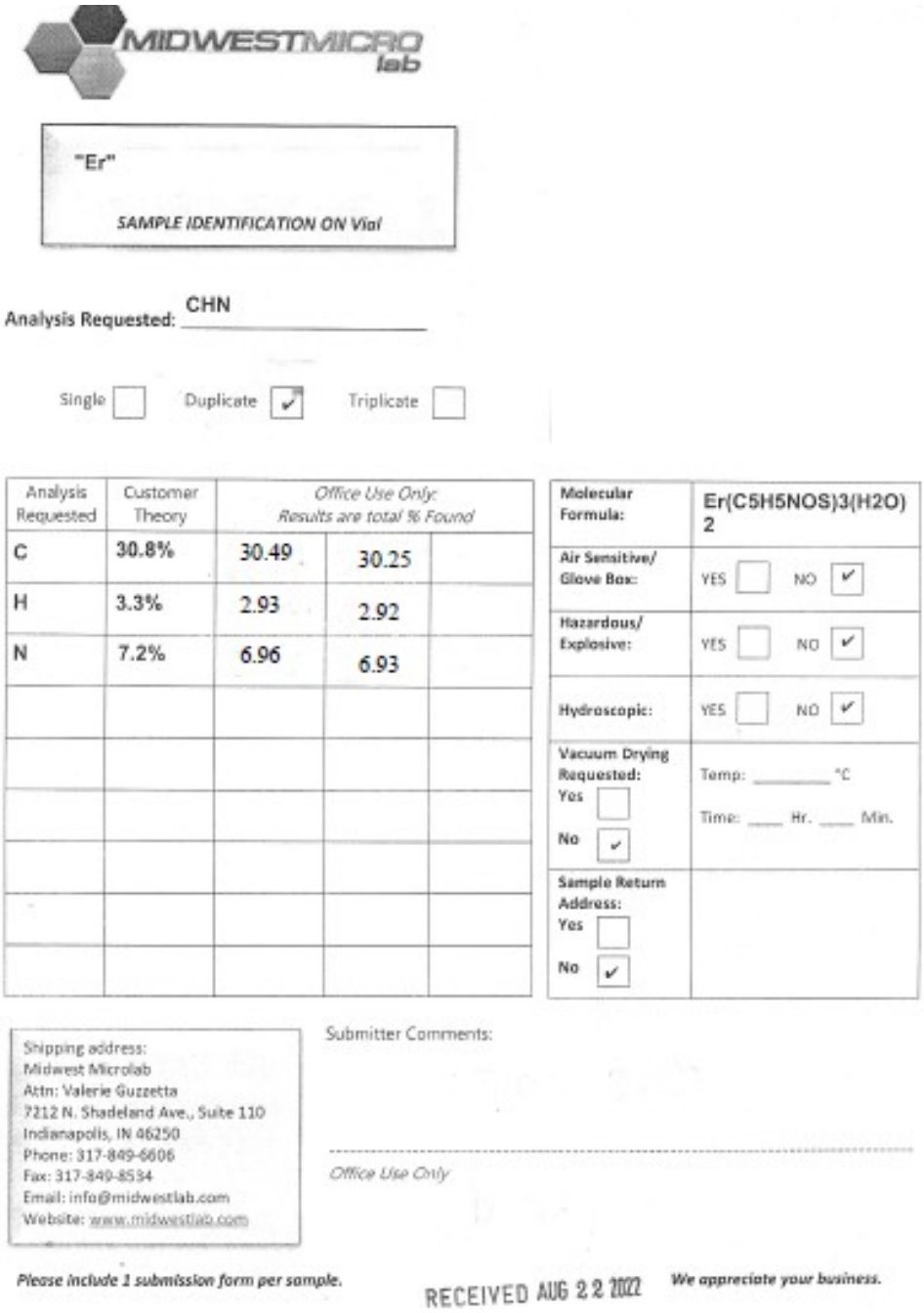

MIDWESTMICRO lab

"Er"

SAMPLE IDENTIFICATION ON Vial

Analysis Requested: CHN

Single ☐ Duplicate ☑ Triplicate ☐

Analysis Requested	Customer Theory	Office Use Only: Results are total % Found		
C	30.8%	30.49	30.25	
H	3.3%	2.93	2.92	
N	7.2%	6.96	6.93	

Molecular Formula:	Er(C5H5NOS)3(H2O)2
Air Sensitive/ Glove Box:	YES ☐ NO ☑
Hazardous/ Explosive:	YES ☐ NO ☑
Hydroscopic:	YES ☐ NO ☑
Vacuum Drying Requested: Yes ☐ No ☑	Temp: _____ °C Time: ___ Hr. ___ Min.
Sample Return Address: Yes ☐ No ☑	

Shipping address:
Midwest Microlab
Attn: Valerie Guzzetta
7212 N. Shadeland Ave., Suite 110
Indianapolis, IN 46250
Phone: 317-849-6606
Fax: 317-849-8534
Email: info@midwestlab.com
Website: www.midwestlab.com

Submitter Comments:

Office Use Only

Please include 1 submission form per sample.

RECEIVED AUG 22 2022

We appreciate your business.

Figure S33: CHN Analysis of **2-Er**.

"Tm"

SAMPLE IDENTIFICATION ON Vial

Analysis Requested: CHN

Single ☐ Duplicate ☑ Triplicate ☐

Analysis Requested	Customer Theory	*Office Use Only: Results are total % Found*		
C	30.7%	30.82	30.56	
H	3.3%	2.89	2.96	
N	7.2%	7.02	6.86	

Molecular Formula:	Tm(C5H5NOS)3 (H2O)2
Air Sensitive/ Glove Box:	YES ☐ NO ☑
Hazardous/ Explosive:	YES ☐ NO ☑
Hydroscopic:	YES ☐ NO ☑
Vacuum Drying Requested: Yes ☐ No ☑	Temp: _____ °C Time: ____ Hr. ____ Min.
Sample Return Address: Yes ☐ No ☑	

Shipping address:
Midwest Microlab
Attn: Valerie Guzzetta
7212 N. Shadeland Ave., Suite 110
Indianapolis, IN 46250
Phone: 317-849-6606
Fax: 317-849-8534
Email: info@midwestlab.com
Website: www.midwestlab.com

Submitter Comments:

Office Use Only

Please include 1 submission form per sample.

RECEIVED AUG 22 2022

We appreciate your business.

Figure S34: CHN Analysis of **2-Tm**.

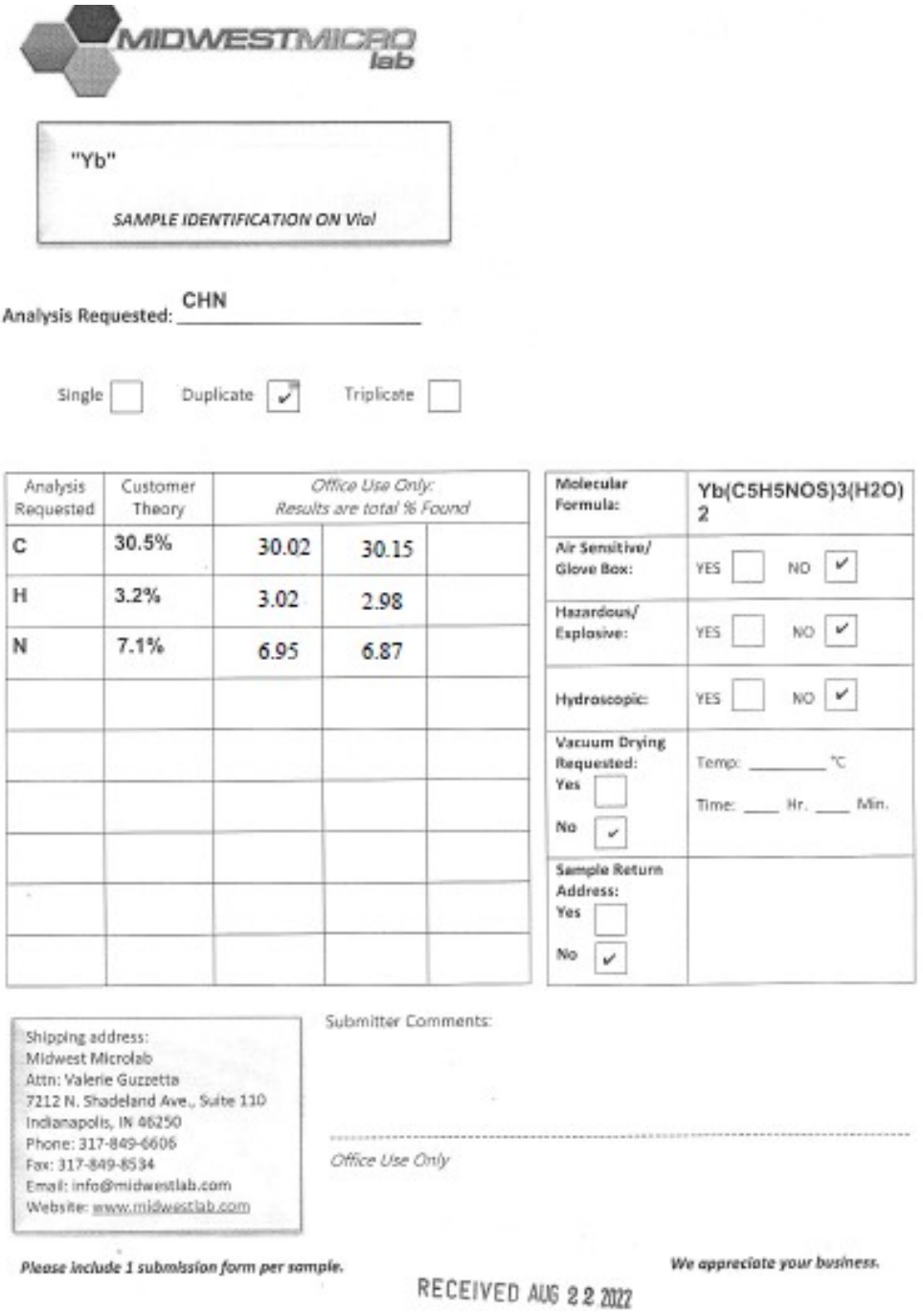

MIDWESTMICRO lab

"Yb"

SAMPLE IDENTIFICATION ON Vial

Analysis Requested: CHN

Single ☐ Duplicate ☑ Triplicate ☐

Analysis Requested	Customer Theory	*Office Use Only: Results are total % Found*		
C	30.5%	30.02	30.15	
H	3.2%	3.02	2.98	
N	7.1%	6.95	6.87	

Molecular Formula:	Yb(C5H5NOS)3(H2O)2
Air Sensitive/ Glove Box:	YES ☐ NO ☑
Hazardous/ Explosive:	YES ☐ NO ☑
Hydroscopic:	YES ☐ NO ☑
Vacuum Drying Requested: Yes ☐ No ☑	Temp: _____ °C Time: ____ Hr. ____ Min.
Sample Return Address: Yes ☐ No ☑	

Shipping address:
Midwest Microlab
Attn: Valerie Guzzetta
7212 N. Shadeland Ave., Suite 110
Indianapolis, IN 46250
Phone: 317-849-6606
Fax: 317-849-8534
Email: info@midwestlab.com
Website: www.midwestlab.com

Submitter Comments:

Office Use Only

Please include 1 submission form per sample.

We appreciate your business.

RECEIVED AUG 22 2022

Figure S35: CHN Analysis of **2-Yb**.

MIDWESTMICRO lab

"Lu"

SAMPLE IDENTIFICATION ON Vial

Analysis Requested: CHN

Single ☐ Duplicate ☑ Triplicate ☐

Analysis Requested	Customer Theory	*Office Use Only: Results are total % Found*		
C	30.4%	30.22	30.36	
H	3.2%	2.91	2.92	
N	7.1%	6.97	6.76	

Molecular Formula:	Lu(C5H5NOS)3(H2O)2
Air Sensitive/ Glove Box:	YES ☐ NO ☑
Hazardous/ Explosive:	YES ☐ NO ☑
Hydroscopic:	YES ☐ NO ☑
Vacuum Drying Requested: Yes ☐ No ☑	Temp: _____ °C Time: ____ Hr. ____ Min.
Sample Return Address: Yes ☐ No ☑	

Shipping address:
Midwest Microlab
Attn: Valerie Guzzetta
7212 N. Shadeland Ave., Suite 110
Indianapolis, IN 46250
Phone: 317-849-6606
Fax: 317-849-8534
Email: Info@midwestlab.com
Website: www.midwestlab.com

Submitter Comments:

Office Use Only

Please include 1 submission form per sample. RECEIVED AUG 2 2 2022 ***We appreciate your business.***

Figure S36: CHN Analysis of **2-Lu**.

References

1 APEX3. Bruker AXS, Inc.: Madison, WI 2017.

2 Sheldrick, G. M. Crystal Structure Refinement with SHELXL. *Acta Crystallogr. C* 2015, **71**, 3-8.

3 Sheldrick, G. M. SHELXT - Integrated Space-Group and Crystal-Structure Determination. *Acta Crystallogr. A* 2015, **71**, 3-8.

4 G. te Velde, F. M. Bickelhaupt, E. J. Baerends, C. Fonseca Guerra, S. J. A. van Gisbergen, J. G. Snijders and T. Ziegler, *J Comp. Chem.* 2001, **22**, 931–967.

5 Lenthe, E. van; Baerends, E. J.; Snijders, J. G. Relativistic Regular Two-component Hamiltonians. *J. Chem. Phys.* 1993, **99**, 4597–4610.

6 Glendening, E. D.; Landis, C. R.; Weinhold, F. NBO 6.0 : Natural Bond Orbital Analysis Program. *J. Comput. Chem.* 2013, **34**, 1429–1437.

7 Ramanantoanina, H.; Urland, W.; Cimpoesu, F.; Daul, C. *Phys. Chem. Chem. Phys.* 2013, **15**, 13902-13910.

8 Binnemans, K.; Srller-Walrand, C. G. *Chem. Phys. Lett.* **1995**, *235*, 163–174.

9 Liu, G. K.; Jensen, M. P.; Almond, P. M. *J. Phys. Chem. A* **2006**, *110* (6), 2081–2088.